



Universiteit Utrecht

Faculty of Science

# Parton and Jet characterisation of gluon splittings to heavy quarks in $pp$ collisions using PYTHIA and VINCIA

BACHELOR THESIS PHYSICS & ASTRONOMY

*Yonne Lourens*

Institute for Gravitational and Subatomic Physics

*Supervisor:*

Dr. Marta Verweij  
Institute for Gravitational and Subatomic Physics

*Daily supervisor:*

MSc. Bas Hofman  
Institute for Gravitational and Subatomic Physics

June 15, 2021

## Abstract

Quantum Chromodynamics (QCD) describes the interaction between gluons and quarks, together called partons. Unfortunately the behaviour of the partons cannot be directly measured by a detector. The Quark–Gluon Plasma (QGP), created in high-energy nuclear collisions, can be studied by measuring the remnants of the hard scattered particles. They decay in jets, collimated sprays of particles, which in turn can say something about the initial partons. In this thesis hard scattering events were generated with Pythia8 and Vincia. Different samples with a gluon as the mother particle were compared by filtering light quark splits, charm/beauty quark splits and gluon splits respectively.<sup>1</sup>

On parton level one can observe that a mother parton with higher  $p_t$  is negatively correlated with the angle between its corresponding daughters. For higher  $\hat{p}_t$  one can distinguish easier  $g \rightarrow q\bar{q}$  from  $g \rightarrow gg$  splits using Vincia. For a more evenly distributed  $p_t$  between daughters  $a, b$  in a  $g \rightarrow ab$  split is the angle between the daughters smaller than for less evenly distributed  $p_t$ . Furthermore the angle between the daughters drops  $\sim 1/z$  for small  $z$  for events in both generators and for the whole  $z$ -spectrum only in Pythia8. Also the events generated with Vincia do not obey the LO kernel splitting functions for  $z \rightarrow 0.5$ .

With a jet matching algorithm matched/unmatched jets are distinguished and correlated with the corresponded daughters and mothers using profile plots. On average we see that the matched jet width and the matched jet mass of  $g \rightarrow gg$  splits is greater than for gluon to quark splits. This means that we can differentiate the two samples from each other by looking at those observables. We observed that the angle between the matched jets and the angle between the corresponding matched daughters is positively correlated. Furthermore in Vincia we observe a 'threshold' in the transverse momentum of matched daughters for which daughters are found in the same jet. We see that for daughters with around  $p_t < 75$  GeV are on average more found in jets with twice the momentum than daughters with higher  $p_t$ . At last for higher daughter  $p_t$  one can conclude that there radiate more particles closely around the daughter than for a daughter with lower  $p_t$ , since for the latter both the jet width and the jet mass are less. The last two measurements apply to all gluon splits (see footnote).

---

<sup>1</sup>Splits of the sort  $g \rightarrow q\bar{q}$  where  $q$  is  $u, d, s$ ,  $g \rightarrow q\bar{q}$  where  $q$  is  $c, b$  and  $g \rightarrow gg$  respectively.

# Contents

<b>1</b>	<b>Introduction</b>	<b>1</b>
<b>2</b>	<b>Quantum Field Theory</b>	<b>2</b>
2.1	Quantum Chromo Dynamics (QCD) . . . . .	2
2.1.1	General Background . . . . .	2
2.1.2	Quark Gluon Plasma . . . . .	3
2.1.3	Splitting functions . . . . .	4
2.2	Jets . . . . .	5
2.2.1	Jet characteristics . . . . .	5
2.2.2	Jet observables . . . . .	6
2.3	The Large Hadron Collider (LHC) . . . . .	7
<b>3</b>	<b>Experimental Setup</b>	<b>8</b>
3.1	The Pythia and Vincia sample . . . . .	8
3.2	Jet Matching Algorithm . . . . .	10
<b>4</b>	<b>Results</b>	<b>11</b>
4.1	Parton level results . . . . .	11
4.1.1	Event generation . . . . .	11
4.1.2	Splitting functions . . . . .	12
4.1.3	Parton quantities . . . . .	15
4.1.4	Correlations between parton quantities . . . . .	17
4.2	Jet level results . . . . .	19
4.3	Parton-Jet correlation results . . . . .	24
<b>5</b>	<b>Conclusion</b>	<b>28</b>
<b>6</b>	<b>Discussion and outlook</b>	<b>29</b>
<b>A</b>	<b>Appendix A</b>	<b>33</b>

# 1 Introduction

In the last decades, the study of the subatomic world has been of great importance. Not only does it allow to better understand the fundamental forces of nature, but also the beginning of the universe we live in. The heart of subatomic physics is the Standard Model of Particle Physics (SM) which describes all the elementary particles where matter and anti-matter are made of [5]. In the early universe both the temperature and density were extremely high ( $T > 100$  GeV) such that all the known particles from the SM were in an thermalized state. Even the particles which interact via the strong force, i.e. quarks and gluons, would have interacted weakly due to asymptotic freedom. Asymptotic freedom is a property of some (gauge) theories that causes the interaction between particles to become weaker as the length scale decreases and the corresponding energy scale decreases [3]. This was thus a hot system where only color-charged particles would interact, a quark-gluon plasma (QGP) [6]

To study the QGP, heavy nuclei are collided at ultra-relativistic energies in the Large Hadron Collider (LHC) at CERN [6]. In such a collision, the temperature is extremely high that the heavy nuclei melt for a very short period of time. Since the temperature cools down very quickly it is very difficult to study the QGP during its life span by direct measurement [1]. However during this short existence, partons (quarks and gluons) traverse the plasma and fragment into sprays of particles, called jets. These jets interact with the QGP and lose energy due to these interactions, which is called jet quenching [7].

The measurements of the remnants of the proton-proton (p-p) and lead-lead (Pb-Pb) collisions at the LHC are performed with the ALICE detector at CERN [8][9]. The properties of these jets will provide information about the particles inside the jets. The focus of this thesis is to compare the properties of the different type of jets. We do this by looking at jets where the initial parton, a gluon mother, splits into a quark-antiquark pair ( $g \rightarrow q\bar{q}$ ). Our comparison is between the different type of daughter quark pairs, where we compare heavy quark samples (charm/beauty) with lighter quark pairs (up/down/strange) and the inclusive sample. Furthermore we will compare two hard scattering samples in a vacuum generated by the generators PYTHIA[4] and VINCIA[25] and look how fundamental differences between these generators result in different measurements.

Our main goal of this thesis is to provide input about how we can differentiate heavy quark splittings from a gluon mother parton and lighter quark splittings when looking at jet measurements. Furthermore with observations about how different matched jets behave with different transverse momentum and different matched quark daughter, we can provide insight about how the matched daughters on parton level themselves behave, since we cannot observe the latter directly in ALICE. [9]

## 2 Quantum Field Theory

### 2.1 Quantum Chromo Dynamics (QCD)

#### 2.1.1 General Background

Quarks and gluons, together called partons, are elementary particles and are part of the Standard Model of Particle Physics (SM) [5]. Quantum Chromodynamics is a comprehensive and well tested theory that describes the behaviour of partons and the interaction between them. QCD has some similarities with Quantum electrodynamics (QED), however QED only deals with one type of charge, which is the electric charge. In QCD are instead of QED three different kinds of charges named color charges. The color charges have nothing to do with visible color that we see as humans. Just like the electric charge, color charge has the property that it is conserved in all physical processes. In QED the photons, the force carrier, mediates the interactions whereas in QCD the massless gluons are its force carriers. Just like a photon responds to an electric charge, a gluon responds to the presence of color charge. However gluons themselves carry color charge, whereas the photons are neutral in electric charge [10]. This means that gluons, unlike photons, can interact with themselves.

Besides gluons, quarks are the only other species of elementary particles that carry color charge. Quarks are spin-1/2 particles that carry a fractional electric charge. Just six different quark 'flavors' are known at the moment, namely: up, down, strange, charm, beauty and top. Only the up and down quarks play a significant role in ordinary matter. The four remaining quarks are a lot heavier and are more unstable. In this thesis we compare samples with up, down and strange quarks to samples with charm and beauty quarks. Although the probability of a gluon splitting into a top anti-top quark pair is really low, we filter these away in both samples to not cause any background.

As already mentioned, gluons themselves are able to carry unbalanced color charge whereas photons can't carry electric charge. Therefore gluons can interact with themselves. In total there are eight physical gluon states forming a color SU(3) octet. SU(3) is a Lie Group that describes the symmetry in color. Furthermore we can summarize QCD by its gauge invariant Lagrangian [10]:

$$\mathcal{L}_{QCD} = \bar{\phi}_i (i(\gamma^\mu D_\mu)_{ij} - m\delta_{ij}) \phi_j - \frac{1}{4} G_{\mu\nu}^a G_a^{\mu\nu} \quad (2.1)$$

$$G_{\mu\nu}^a = \partial_\mu \mathcal{A}_\nu^a - \partial_\nu \mathcal{A}_\mu^a + g f^{abc} \mathcal{A}_\mu^b \mathcal{A}_\nu^c \quad (2.2)$$

$$D_\mu = \partial_\mu - iqA_\mu \quad (2.3)$$

where  $\phi_i(x)$  is the quark field,  $\mathcal{A}$  the gluon field and  $m_j$  the quark masses. The strong force, the force between the partons, is described by this equation completely.

One of the most important theoretical discoveries in QCD is that the strength of the force (described by the coupling constant) between the quarks and gluons, unlike other forces in nature, gets weaker at short distances. Similarly this means that the interactions between

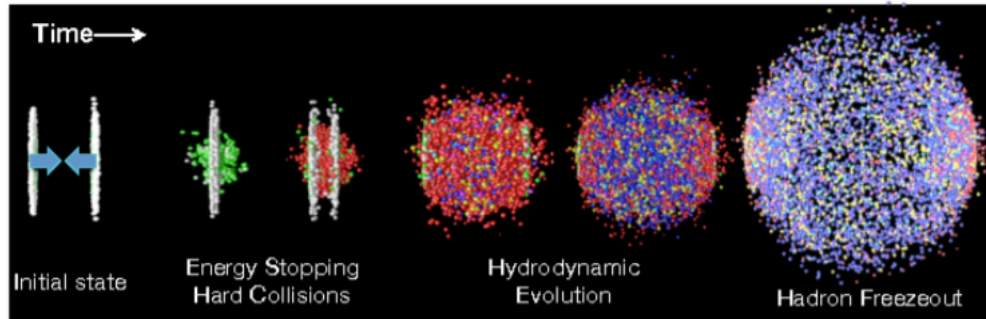


Figure 1: Evolution of the QGP

the partons get stronger with increasing distances. As a result of this behaviour the gluons become asymptotically free at shorter distances. Moreover they behave as quasi-free particles inside hadrons. Another very important concept in QCD is confinement [10]. Gluons and quarks are never observed freely in nature but are usually bound together to form baryons (three quarks) or mesons (two quarks) particles.

However a question that arises is: "Why do we observe jets instead of simple particles in for example p-p collisions. This is because of the strength of the gluons significantly depends on the energy and momentum of the gluon. Gluons that carry a lot of momentum couple weakly whereas a less energetic gluon couple strongly. This means that fast moving quarks or gluons rarely emit radiation in the form of a gluon, which is why the jets are collimated flows of particles. On the other hand there also could be a lot of soft radiation from slow gluons, which is the reason there are many particles inside a jet or parton shower.

### 2.1.2 Quark Gluon Plasma

The Quark Gluon Plasma (QGP) is a state of matter that is formed in heavy-ion collisions at high centre of mass energy. In the QGP the confinement of the partons changes, such that it is possible to move freely without being confined. Also a characteristic of the QGP is that it has almost zero viscosity, which means that partons inside the QGP are completely unhindered to move. This makes it an interesting field of study. The QGP can be formed when hadronic gas undergoes a phase transition. In Fig. 1 the evolution of the QGP is shown. One can see that initially it grows fast, since there is a lot of internal energy and thus is the temperature very high. However when it expands, the temperature drops and the partons will again hadronize to mesons or baryons. Whenever a quark or gluon in a parton jet passes through the QGP it loses some of its energy due to interactions with the partons inside the QGP. This effect is called Jet quenching.

One interesting observation that is made, is that there is a lot less jet quenching for quark jets with quarks with a higher mass, like beauty or charm quarks. However the interactions of QCD are flavour blind, i.e. gluons couple only to the color charge to quarks, meaning that there seems no fundamental difference between light and heavy quark dominated jets. One of the explanations of the former observation, is that a quark mass introduces a constraint on radiation phase space. And thus it suppresses the vacuum as well as the medium induces QCD radiation [14]. This is known as the 'Dead cone effect' and led to the expectation that

heavy quarks should lose less energy due to interactions with the QGP than lighter quarks would. Several other explanation are made in [14].

### 2.1.3 Splitting functions

The jet evolution, or the branching of the parton shower are governed by QCD radiation probabilities given by the Dokshitzer-Gribov-Liaptov-Altarelli-Parisi (DGLAP) equations [11] [12]. The equations describe the branching of the parton shower in a vacuum. The equations are coupled integro-differential equations with splitting functions as kernel elements [11]. These splitting functions  $P_{ab}(z)$  describe, for  $z < 1$ , the probability of finding a parton of type  $a$  from a parton of type  $b$  carrying a fraction  $z$  of the longitudinal momentum of  $b$ . Fundamentally PYTHIA and VINCIA differ since VINCIA also takes on next to leading order (NLO) calculations whereas PYTHIA only takes on leading order (LO) calculations. At LO, we have four splitting functions listed in Fig. 2 with their associated Feynman diagrams [11]. where  $C_F = \frac{4}{3}$ ,  $C_A = N_C = 3$  and  $T_R = \frac{1}{2}$ . We will check that events generated

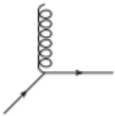

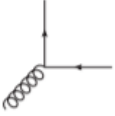
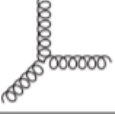
Diagram	Splitting Function
	$P_{qq}^{(0)}(x) = C_F \left[ \frac{1+x^2}{(1-x)_+} + \frac{3}{2}\delta(1-x) \right]$
	$P_{gq}^{(0)}(x) = C_F \left[ \frac{1+(1-x)^2}{x} \right]$
	$P_{gg}^{(0)}(x) = T_F [x^2 + (1-x)^2]$
	$P_{gg}^{(0)}(x) = 2C_A \left[ \frac{1-x}{x} + x(1-x) + \frac{x}{1-x_+} \right] + \delta(1-x) \frac{11C_A - 4T_F n_f}{6}$

Figure 2: Leading order splitting functions and associated diagrams. [11]

in PYTHIA will satisfy these splitting function, whereas VINCIA will not. Higher order contributions to the splitting functions have been calculated in [12][13]. In Fig. 3 are for example the Feynman diagrams shown for NLO contributions in  $g \rightarrow gg$  (left) and  $q \rightarrow qq$  (right) splits.

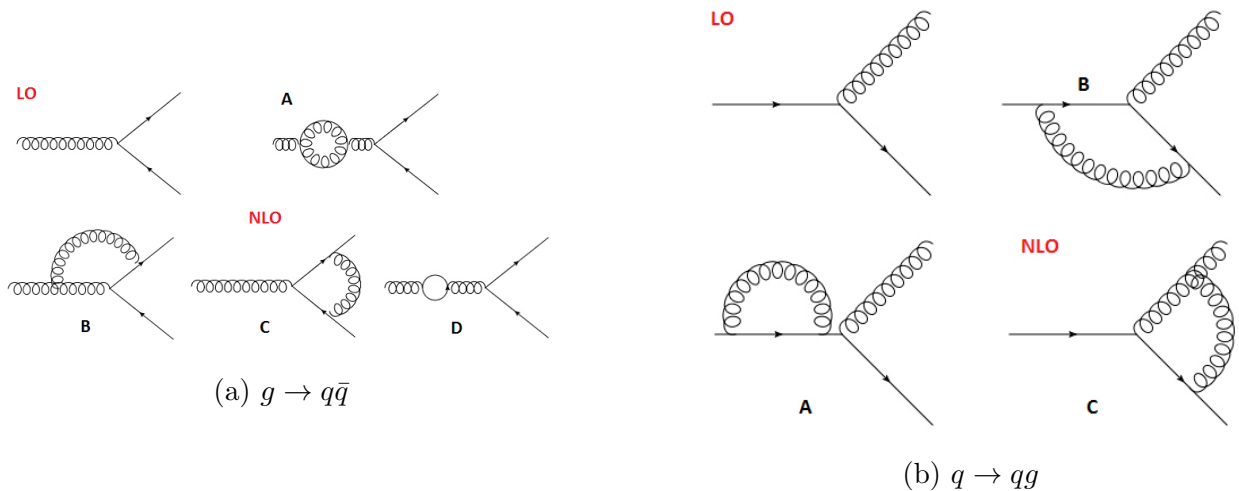


Figure 3: Feynman diagrams of NLO calculations for  $g \rightarrow gg$  (left) and  $q \rightarrow qq$  (right) splits. [28]

Since it is quite difficult to plot higher order splitting functions we won't be checking VINCIA's NLO calculations. To check the NLO corrections in Vincia we need to follow the NLO radiations in the generator. We do not do this since we only follow two daughters while NLO will result in three. If we have medium to deal with, we also need to take medium-induced branching evolution into account.

## 2.2 Jets

### 2.2.1 Jet characteristics

Instead of using energy and polar coordinates we use in collider kinematics pseudo-rapidity  $\eta$ , the azimuthal angle  $\phi$  and mass  $m$  as coordinates to describe particles in a collision. Shown in Fig. 7 is a sketch a typical detector in Cartesian coordinates. If we take the  $z$  axis to be the beam axis we can define  $p_T$  and  $\phi$  as the modulus and the azimuthal angle in the transverse plane, thus

$$p_T = \sqrt{p_x^2 + p_y^2} \quad (2.4)$$

and

$$\phi = \arctan\left(\frac{p_y}{p_x}\right). \quad (2.5)$$

From the figure one can see the polar angle  $\theta$ , the angle between the particle and the beam. This angle defines the pseudo-rapidity  $\eta$ , which we also can define as the modulus of the 3-momentum. This yields

$$\eta = -\log\left(\tan\frac{\theta}{2}\right) = \frac{1}{2}\log\left(\frac{|\vec{p}| + p_z}{|\vec{p}| - p_z}\right). \quad (2.6)$$



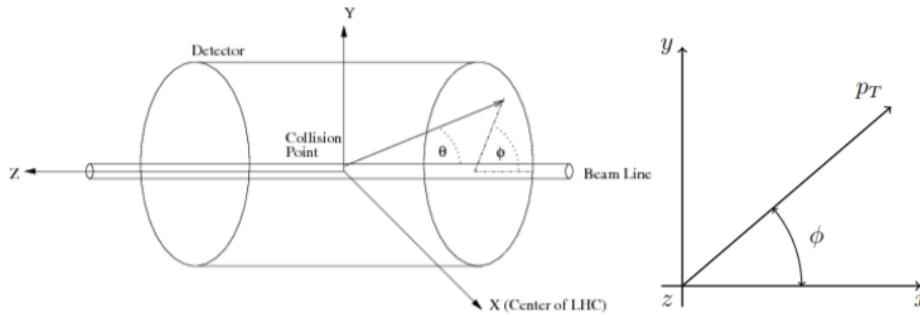


Figure 4: Schematic overview of coordinates in a collider detector [24].

In words this means that if a particle moves in the direction of the beam axis, so  $\theta = 0$ , we have  $\eta = \infty$  and if a particle moves away with a right angle with respect to the collided particles, we have  $\eta = 0$ . Furthermore we can define rapidity as

$$y = \frac{1}{2} \log \left( \frac{E + p_z}{E - p_z} \right). \quad (2.7)$$

In contrast to the pseudo-rapidity,  $y$  is mainly theoretically used (bron) instead in experiments where mainly  $\eta$  is used. For this we will also use  $\eta$ . With the rapidity  $y$  and the azimuthal angle  $\phi$  we can describe the angle between two particles by

$$\Delta R_{ij} = \sqrt{\Delta \eta_{ij}^2 + \Delta \phi_{ij}^2} \quad (2.8)$$

where  $i, j$  are subscripts of two different particles. All the measured particles will be grouped and matched in jets by jets algorithms which will be explained in section 3.2. Similarly the jets are described by  $p_T, \eta, \phi$  and  $m$ . In Fig. 5 is a schematic overview given of the type of split we are interested in.

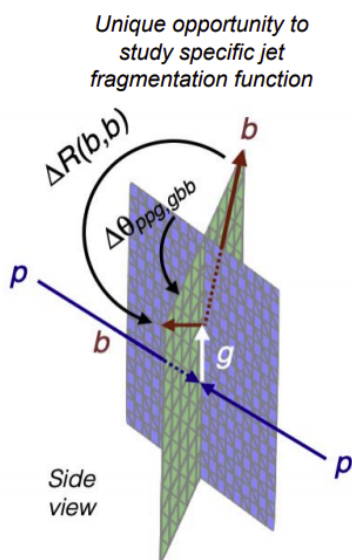


Figure 5: Schematic overview of a typical  $g \rightarrow b\bar{b}$  split [26].

### 2.2.2 Jet observables

Within each jet itself is a substructure that has different internal properties, or jet observables. To compare the jets from a certain filtered sample in PYTHIA with other filtered samples and with VINCIA, we need properties of the jets produced in the different samples. We look at different jet substructure observables. These observables are given by [15]

$$\lambda_\beta^\kappa = \sum_{i \in \text{jet}} z_i^\kappa \left( \frac{R_i}{R_0} \right)^\beta \quad (2.9)$$

These observables  $\lambda_\beta^\kappa$  are called generalized angularities, which depend on an angular component  $\beta \geq 0$  and the energy weighting factor  $\kappa \geq 0$ . Here  $z_i$  is the momentum fraction of the

particle,  $R_i$  the azimuthal angle with respect to the beam axis and  $R_0$  is the radius of the jet. Different values of  $(\beta, \kappa)$  give different observables. In this thesis we are only interested in the width of the jet and the jet fragmentation distribution. These are the observables with  $(\beta, \kappa) = (1, 1)$  and  $(0, 2)$  respectively. We could also calculate the observables by

$$W = \frac{\sum_i \Delta R_i p_{T,i}^2}{\sum_i p_{T,i}^2} \quad (2.10)$$

as the jet width and the jet fragmentation distribution  $p_T D$  is calculated by

$$p_T D = \frac{\sqrt{\sum_i p_{T,i}^2}}{\sum_i p_{T,i}^2} \quad (2.11)$$

where the sum runs over the jet constituents. This variable takes values between zero and one, where higher values are taken by quark-jets. This variable provides a very good discrimination for the full  $p_T$  spectrum [16]. Since we differentiate our samples in three categories, i.e. the sample where daughters are lighter quarks, charm/beauty quark and the inclusive sample, we can see how these variable changes according to each sample. The last observable we will introduce is the jet mass which can be calculated with

$$M^2 = \left( \sum_i E_i \right)^2 - \left( \sum_i \vec{p}_i \right)^2. \quad (2.12)$$

The jet mass  $M$  is closely related to the virtuality of the parton that initiated the jet [27]. The jet mass  $M$  is closely related to the virtuality of the parton that initiated the jet and is defined as:[8]

### 2.3 The Large Hadron Collider (LHC)

In Geneva, at CERN particles are collided in the Large Hadron Collider (LHC) (bron). The LHC is the most powerful and largest particle accelerator in the world. With the use of superconducting magnets two high energetic particle beams are accelerated to a speed near the speed of light. Once the particles reach this velocity, we collide them in one of four detectors, ATLAS, ALICE, LHCb or CMS.

In Fig. 6 one can see where at CERN the different experiments are being conducted. CMS is one of the four experiments which is dedicated to the detection of heavy-ion collisions. The ALICE detector however, is specialized in finding and proving the existence of the QGP by looking at collisions of particles. In each of these experiments there are different detectors determining different properties, for example at the particle's momentum, energy or charge. All these detectors are layered around the detection point.

In this thesis however, we will not use actual data from these experiments, but will work with samples that are generated such

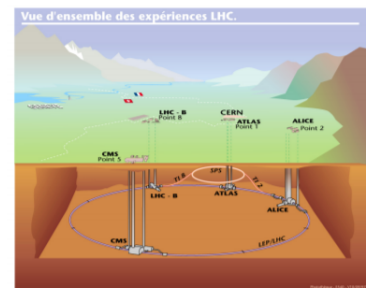


Figure 6: Overview of the LHC at CERN in Geneva [22]

that it resembles a real particle collision, since the generators are fine-tuned by experimental results.

### 3 Experimental Setup

To generate events like the collisions done at the LHC, the event generators PYTHIA and VINCIA are used. These generators simulate the collisions at high energies between the elementary particles. Both generators contain the theory and models based on theoretical insight and are fine-tuned with experimental results. One main difference between the two is that VINCIA incorporates both the collinear and the soft limit of QCD matrix elements at leading colour. Hence VINCIA should exhibit improved colour-coherence effects relative to PYTHIA's simple shower model [25]. While both generators are based on QCD, none of these take jet quenching into account. We discuss this some more in the discussion and outlook section.

The results of the generators simulate events that are like the experimental results, however this is only done on parton level. In addition, the generators also have a hadronization model. So the parton shower has at the end partons which are then hadronized in the generators to form hadrons. Hadronization is a non-perturbative process (low energy scale) so it is modeled and not precisely calculated. In both generators this is done with the Lund string hadronization model [2]. The hadronization method is the same for PYTHIA and VINCIA. Thus what is known are the momentum and energy of the final particles. But these particles are not yet assigned to jets. With the software package FastJet [20] [21] we can apply the sequential recombination algorithm explained in section 3.2 to assign each particle to a jet. The distance measures in this algorithm are given by'

$$d_{ij} = \min(1/p_{T_i}^2, 1/p_{T_j}^2) \Delta R_{ij}^2 / R^2 \quad (3.1)$$

$$d_{iB} = 1/p_{T_i}^2 \quad (3.2)$$

where we have  $p_T$  as defined in equation 2.4 and  $\Delta R$  angle between the two particles, defined as in equation 2.8. To analyse this we use ROOT. ROOT [18] is a C++ based framework developed at CERN which is used for data analysis, statistical analysis, storage and visualisation. ROOT can take the input of FastJet, and together with the events generated by PYTHIA and VINCIA we can analyse all of our data with ROOT and visualize it with Python3.

#### 3.1 The Pythia and Vincia sample

Since Pythia and Vincia are only different on higher order matrix elements, will explain only how the Pythia sample was prepared Pythia. The Vincia is similarly prepared. Pythia is again a C++ program used as to generate high energy collisions using modern day QCD, namely unperturbative QCD. The evolution and branching of the particle jets are based on the DGLAP's kernel leading order splitting functions explained in section 2.1.3. In figure 7 is a simplified version of a typical evolution pictured. Since we deal with high energies, we

have that the coupling strength  $\alpha_s$  is small and thus for allows perturbative QCD [1]. Since the QGP is not taken into account in Pythia, it only generates weakly coupled interactions.

Pythia and Vincia both generate hard scattering processes between a few body system.

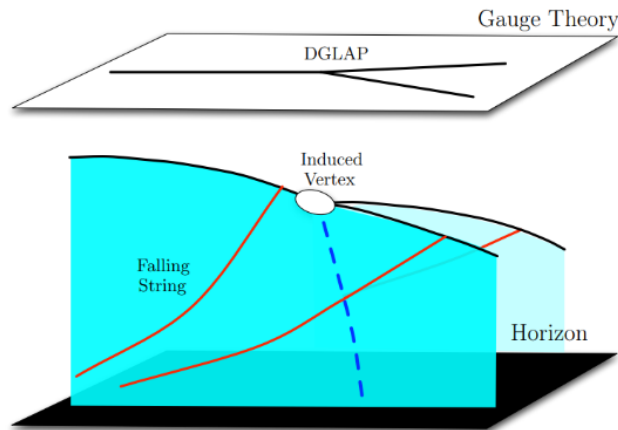


Figure 7: Sketch of the two methods to view the parton shower evolution. As one can see, in the top half is the parton evolution in a vacuum, described and governed by the DGLAP equations. In the lower however, is the evolution of a parton shower pictured when both the weak and the strong coupling interactions are taken into account [23].

Both simulate the interactions the particles have with each other and its outgoing particles. The process is simulated in a vacuum, so no interaction with the QGP was taken into account. Furthermore, we do not look at the interactions with the specific detector materials. Pythia is useful to both study hard and soft QCD processes. In our simulation we chose for the hard QCD process, since this allows jet production above a minimum  $p_T$ . Pythia will not give reliable and justifiable predictions below this  $p_T$ . In Pythia this threshold is 50 GeV for a fixed target beam.

Before an event is generated in Pythia one must choose the number of events generated, the tune and the average  $p_T$  of the initial partons named  $\hat{p}_T$ . We chose 10000, 14 and 120 respectively for both generators. We also ran the same number of events for the average  $p_T$  of 300 GeV and 500 GeV. The tune of the generator is an option where all necessary parameters are stored to predict and use the different physics components. Once we ran the events, the results are stored in a pu14 file. The data that is collected in this file is the 4-momentumvector of each particle and each vertex number. The vertex number of a particle tells something about the identity of the particle in the simulation. In Pythia we have two particle identities, namely -1 which denotes the initial partons and 0 which denotes all the final state particles. Per event two initial partons are generated with the same initial momentum traversing in opposite direction due to energy conservation. In the following paragraph we go into detail on how these particles are clustered into jets and how to match the daughter particles, next generation after the mother partons, to a jet for each event.

For the analysis of the event generation we need different quantities that are saved in ROOT.

For the study on parton level we firstly need the mother its PDG code to see what type of mother particle we have. To force analysis on  $g \rightarrow q\bar{q}$  and  $g \rightarrow gg$  splits, we filter on mother PDG equal to 21 (which is the PDG code of a gluon particle). The PDG codes for up, down, strange, charm, beauty and top quarks are respectively 1, 2, 3, 4, 5, 6, while the anti-quarks are the negative values of these. Since we want to force the splits described above, we want to only analyse the events where the two daughters PDG, in absolute value, differ by zero. This means that for both daughters we have the same quark flavor but with opposite charge. If this is not the case, we continue with the next event. Now with the right mother and daughter particles we can start the analysis. With the daughter particles we can start to jet match, explained in section 3.2 and analyse correlation between daughter quantities on parton level. Furthermore we can distinguish the matched jets from the unmatched jets (so the jets where in the daughter particle does not go), and look for differences in quantities between the two.

### 3.2 Jet Matching Algorithm

In this thesis we use two different algorithms. The first algorithm is used to assign all other particles to a jet. This algorithm is implemented in the Jet Software. For this a sequential recombination algorithm is used:

1. Calculate the distance  $d_{ij}$  between all particle pairs  $i, j$
2. Calculate the jet distance  $d_{iB}$  for all particles  $i$  to the beam  $B$ .
3. Find the smallest distance of  $d_{ij}$  and  $d_{iB}$ . If  $d_{ij}$  is the smallest, combine the particles  $i$  and  $j$  into a new particle. If  $d_{iB}$  is the smallest, call it a jet and remove it from the list/
4. Repeat all steps above until all the particles are clustered into jets.

With this algorithm we can look at correlations between the number of observed hadrons per jet and the different masses for the quark daughter in the splits.

The second algorithm only considers matching the daughter particles to a jet. This is done to see if there is a correlation between observed jets and its matched parton daughter. To determine which daughter should be assigned/matched to each jet, we use a sequential recombination like algorithm. We are only interested in daughter who are in different jets. The one I wrote looks like:

1. First look at the PDG of the daughters and filter accordingly.
2. If Dr Split (saved observable in ROOT), is angle between split, between daughter partons is greater than predetermined  $R = 0.4$  we continue. Otherwise the daughters are in the same jet.
3. Calculate the distance  $\Delta R_{ij}$  between all daughters  $i$  satisfying 1. and 2. and all jets  $j$  per event.

4. Match each daughter particles  $i$  to the jet  $j$  where  $\Delta R_{ij}$  is minimum.

Now one has matched each daughter satisfying 1. and 2. to a jet. We can continue with this algorithm to determine various characteristics of matched jets.

1. Find the index of the jets where  $\Delta R_{ij}$  is minimum.
2. Find with these indices the transverse momentum of the jet  $p_{T_j}$ , azimuthal angle  $\phi_j$  and  $\eta_j$ .
3. Find corresponding mother parton and daughter and see if jets quantities are correlated with parton quantities.
4. To determine non matched jets, we look at the hemisphere both matched jets are in. A non matched jet is also in this hemisphere by forcing  $\phi_{nonmatched} - \phi_{matched_i} < \pi$  for  $i$  the matched jets. Save these unmatched jets in a separate list.

## 4 Results

### 4.1 Parton level results

#### 4.1.1 Event generation

After generating events with the setup explained in section 3.1 we can start the analysis of the ROOT file. Since we want results for different  $g \rightarrow q\bar{q}$  splits and  $g \rightarrow gg$  we need to filter per event accordingly. Since we want to analyse different samples with light and charm/beauty quark splits, we need to distinguish the daughters from each other. We use the method explained in section 3.1 to see how many type of different quark splits there are generated. We filter away the top quark splits, since we do not want to analyse these.

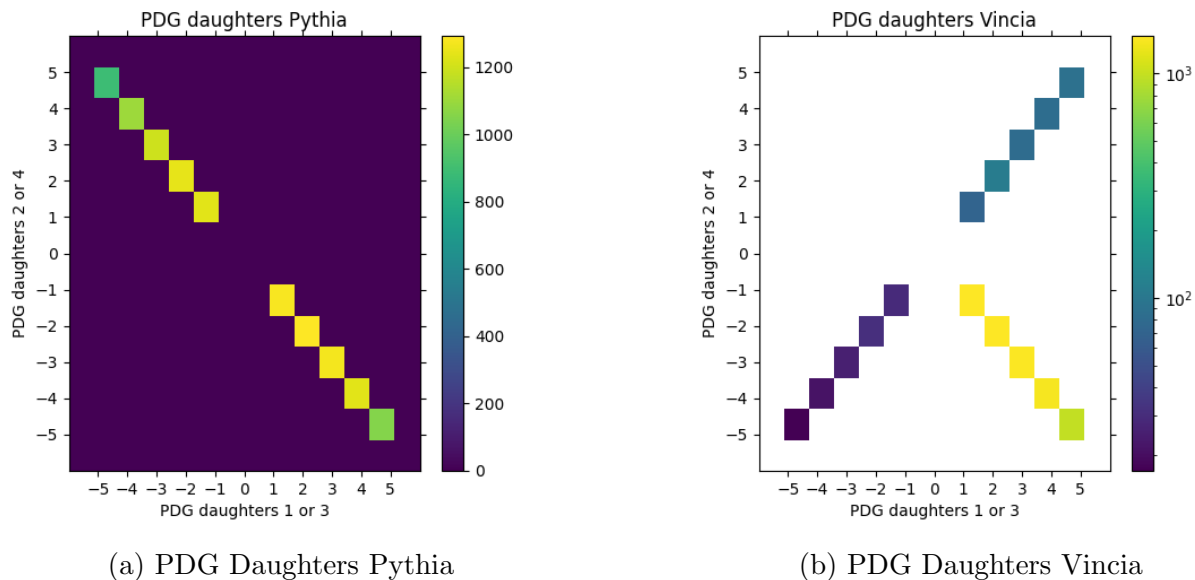
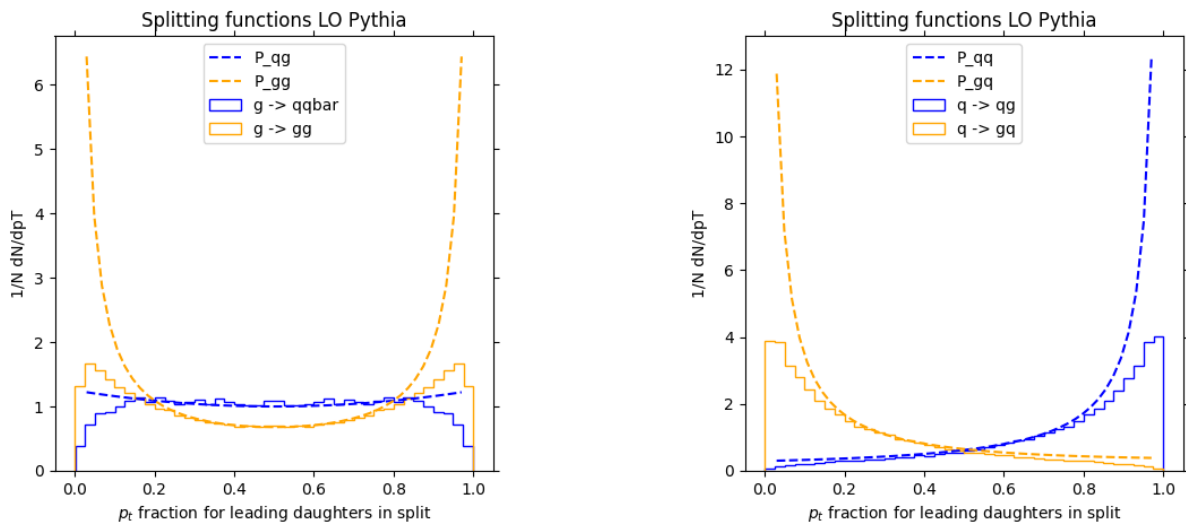


Figure 8: 2D histogram of daughter PDG codes for Pythia (left) and Vincia (right) where we combine mother parton 1 with daughters 1 and 2 and mother parton 2 with daughters 3 and 4. The plot for Vincia has a log z-scale for clarity reasons.

In Fig. 8 we see the results of this plotted in a 2D histogram. We can immediately see a difference between Pythia and Vincia. Pythia’s histogram looks like it should. All daughter pairs have opposite sign in a  $g \rightarrow q\bar{q}$  split and the difference between the daughters PDG is zero (in absolute value). This means that for both daughters we have the same quark flavor but with opposite charge. For Vincia the difference between the PDG of the daughters is also zero, however one can see that there are some splits where the PDG of daughter 1 and 2 or daughter 3 and 4 are the same. When generating these events separately we indeed find that there are a few splits with same daughter PDG. One explanation of this may have to do with the nature of Vincia’s next to leading order calculations. For this to happen we need a gluon where then the gluon is next order in the perturbation theory so part of the NLO matrix elements in Vincia. For example due to the gluon coupling to a  $\bar{q}$  we can get  $qq$ . Before a daughter particle is saved it may be that the daughter’s PDG flips through a strong interaction with itself.

#### 4.1.2 Splitting functions

Next we check if the splits obey the splitting functions explained in section 2.1.3. There are of course many more splitting kernels however for this thesis they are not important.



(a) Splitting functions of  $g \rightarrow q\bar{q}$  (blue) and  $g \rightarrow gg$  (orange) are dashed.

(b) Splitting functions of  $q \rightarrow qq$  (blue) and  $q \rightarrow gq$  (orange) are dashed.

Figure 9: Measurements of leading order splitting functions in density histogram in Pythia. On the x-axis the  $p_t$  fraction of the  $p_t$  sum of the daughters carried by daughter one (first particle after the arrow in the right figure). All histograms are self-normalized and normalized by the bin width.

The results in Pythia are found in Fig. 9. All the following histograms are self-normalized, so only the shape is important. Since Pythia has only leading order (LO) matrix elements, we see that the measurements are fairly similar to the theoretical splitting functions in the interval  $[0.15, 0.85]$ . In the following paragraphs we will highlight a couple of interesting observations.

At first, in the left figure we can see that the splitting functions are symmetrical. One can also deduce this easily by looking at the last two equations in Fig. 2. By indistinguishably we have that the results in the left figure are also symmetrical, since we cannot distinguish two daughter gluons. Furthermore the definition of the third equation in Fig. 2 allows for anti-quark and quark leading daughters resulting in a symmetric result.

Next we can see that in both figures, when approaching 0 or 1 the splitting functions fit the measurements worse. One reason of this is that the splitting functions diverge when  $z \rightarrow 0$  or  $z \rightarrow 1$ . This is why at closer values to these limits the splitting functions are less accurate. Another reason for the inaccuracy is that a split where a daughter has  $p_t$  fraction 0 or 1 is not considered as a particle, since one of the daughters has zero energy. This is why at these values the number of particles drops to zero.

Also worth mentioning is that we use the sum of the daughters  $p_t$  in the split instead of the mother parton to calculate the momentum fraction. This is since the sum of the daughters  $p_t$ , and even the  $p_t$  of one daughter is sometimes greater than the mothers  $p_t$ . We can plot this to make it a bit clearer. The results are given in Fig. 10. We used a grid in the



plot to make it easier to see.

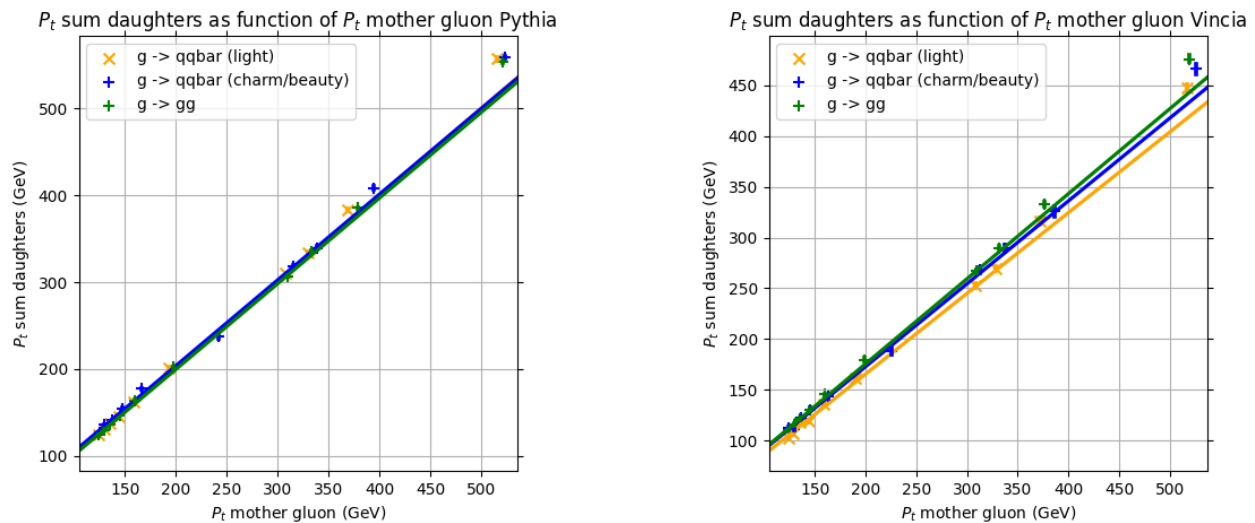
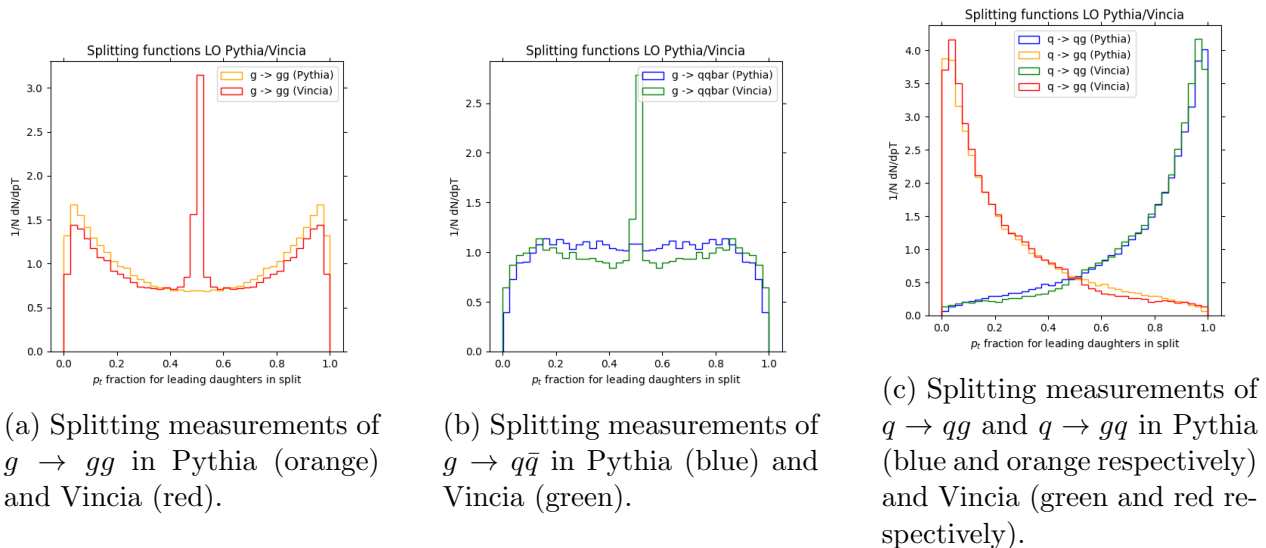


Figure 10:  $p_t$  sum daughters in a split plotted against the  $p_t$  of the mother gluon in Pythia (left) and Vincia (right). Markers indicate calculated averages over all events. We loop through the three different splits we use to compare partons quantities (explained in next paragraph).

We can see that in both generators it is not a straight line. In Vincia we can clearly see that the sum of the daughters  $p_t$  is greater than the  $p_t$  of the mother. One explanation for this to happen is that the daughter particles pick up some initial state radiation (ISR). ISR is the radiation from the incoming partons before the hard scattering between the initial partons takes place.

Next we look at the difference between Pythia and Vincia in splitting measurements.



(a) Splitting measurements of  $g \rightarrow gg$  in Pythia (orange) and Vincia (red).

(b) Splitting measurements of  $g \rightarrow q\bar{q}$  in Pythia (blue) and Vincia (green).

(c) Splitting measurements of  $q \rightarrow qg$  and  $q \rightarrow qq$  in Pythia (blue and orange respectively) and Vincia (green and red respectively).

Figure 11: Measurements of leading order splitting functions in density histogram in Pythia and Vincia. On the x-axis the  $p_t$  fraction of the  $p_t$  sum of the daughters carried by daughter one (first particle after the arrow in the right figure). All histograms are self-normalized and normalized by the bin width.

The results are given in Fig. 11. Immediately we can see differences between splitting kernel measurements of Pythia and Vincia. We see that Vincia does not obey the LO splitting kernels. In this thesis we did not plot the next to leading order (NLO) splitting functions, since they were quite long. This is further discussed in the discussion and outlook section. Since Vincia uses NLO matrix elements we can predict that Vincia obeys NLO splitting functions as well. On other reason for the peaks may be due to the 'double PDG' splits seen in Vincia, discussed in the previous section. However the peak is also seen in  $g \rightarrow gg$  splits, so this only applies for gluon splits (Fig. 11b).

#### 4.1.3 Parton quantities

Now that we have established the behaviour of different splits we can 'zoom in' a bit more. One goal of the thesis is to compare different parton quantities for different samples. As discussed we would like to compare measurements of  $g \rightarrow q\bar{q}$  splits for light quarks and charm/beauty quarks and the inclusive sample. After running the analysis on the inclusive sample it seems more logical to use the  $g \rightarrow gg$  sample. We do this since we can relate the splitting function of the split above to different measurements (we do not have one for the inclusive sample) and a lot of events generate  $g \rightarrow gg$  splits, so we will not be missing much. Thus we will cut loose all quark mother particles and further splits. This is further discussed in the outlook section.

Since we match daughters with jets and we want to correlate mother quantities with the characteristics of jets we only plot 1D histograms of the angle between daughters and the momentum fraction of the daughters. We already treated the  $p_t$  sum of the daughters and the  $p_t$  of the mother above. We plot the  $z$  (momentum fraction) of different quark splits i.e.

we plot  $g \rightarrow q\bar{q}$  splits for the light quark splits and the charm/beauty splits and compare these with the  $g \rightarrow gg$  sample. We do this to see if different quark samples obey the splitting functions above. For the latter we get the 1D distributions

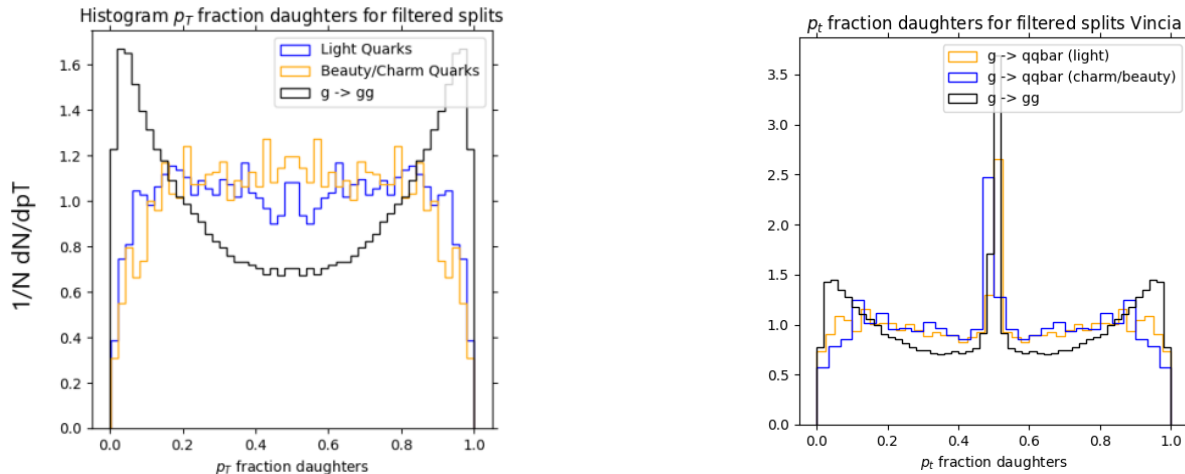


Figure 12: 1D distributions of  $p_t$  fraction daughters in Pythia (left) and Vincia (right) for filtered splits. All histograms are self-normalized and normalized by the bin width.

We already saw in Fig. 9 that the  $g \rightarrow gg$  splits obeys its corresponding splitting function. Furthermore we can see that that heavy quark splits (charm/beauty) fit the figure worse than light quark splits in Pythia. Near  $z = 0.5$  we can also see a difference between light and heavy quarks splits. For the light quark splits we can see a dip around  $z = 0.5$  whereas we do not see this for the heavy quarks. This is perhaps relevant to distinguish since it means that there are relative less daughters in light split quarks with  $p_t$  fraction around  $z = 0.5$  than heavy quarks. One can also see that the drop for  $z \rightarrow 0$  and  $z \rightarrow 1$  start a bit earlier for quark splits than for the gluon split. The latter is not seen in Vincia however. All the histograms are scaled to only study the shape.

Next we study the results of the 1D histograms of the angle between the daughters.

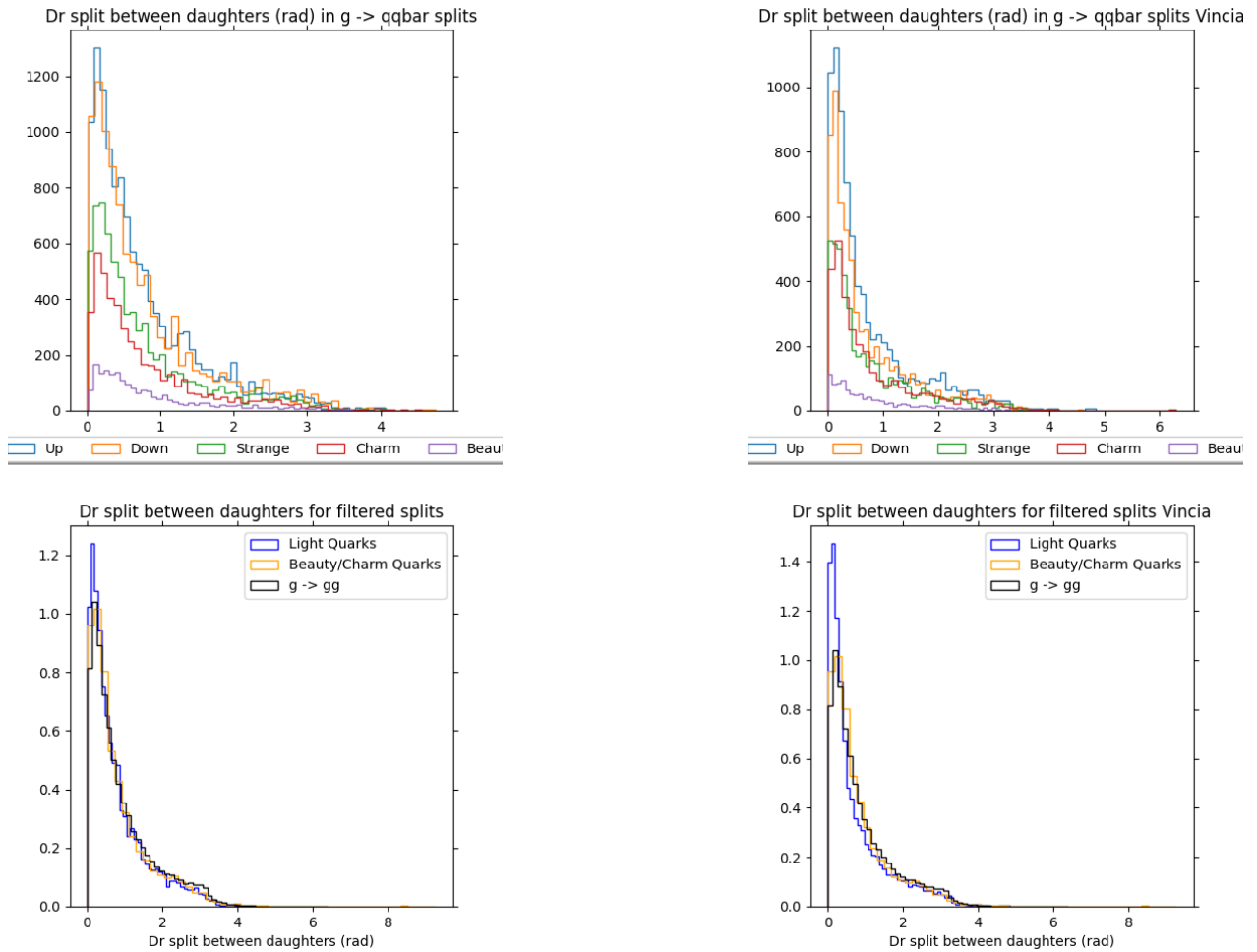


Figure 13: 1D distributions of the angle at parton level between daughters in Pythia (left two figures) and Vincia (right two figures). The top two figures show the results for quark only splits  $g \rightarrow q\bar{q}$ . The bottom two show the results for all for filtered splits together.

As seen in figure 13 we have in the top two figures for all the different quark splits to see if they differ from each other. For Pythia all the quark splits behave fairly similar. As for Vincia one can see the distribution of the beauty quark is more evenly distributed and the peak near parton angle is zero is less clear. This can be due to the lack of beauty quark splits. When looking at the bottom two figures we can see that all type of splits behave fairly similar. This means that we cannot immediately distinguish one sample from the other when looking at the angle between the daughters.

#### 4.1.4 Correlations between parton quantities

Now we want to relate some parton quantities and see if they are correlated. For this we make a profile plot from the 2D histograms made to correlate the two quantities. We make a profile plot by averaging the angle between the daughters as a function of the  $p_t$  of the mother gluon. From QCD it follows that the angle must become smaller when the  $p_t$  gets

higher. We generate also for  $\hat{p}_t$  is 300 GeV and 500 GeV for both generators. The results are

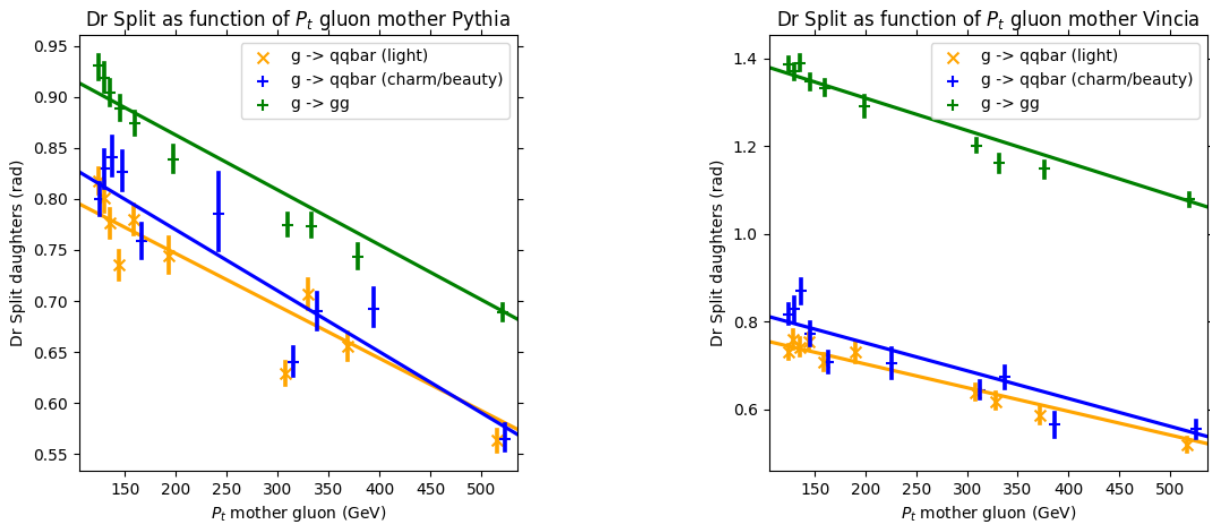


Figure 14:  $p_t$  mother gluon in a split in a profile plot against the the angle at parton level between the daughter particles in Pythia (left) and Vincia (right) for filtered splits. The error bars are standard statistical errors.

given in Fig. 14. One can deduce several features from these plots. First we can see that our prediction for a negative correlation between mother  $p_t$  and the angle between the daughters is correct. This means that for higher  $p_t$  of a mother parton we have a smaller angle between the corresponding daughters. We also distinguish three different splits, and see that light and heavy (charm/beauty) splits have similar behaviour. When looking at the gluon split however, we can see that the average angle at parton level is much larger then for the quark splits. For Vincia the angle at parton level is almost double than the angle at parton level for quark splits. Since Vincia is a more realistic generator this is quite good. However we measure on average and we cannot yet experiment with  $\hat{p}_t$  of 500 GeV. At higher  $p_t$  we can see that both generators will exhibit the same behaviour.

Next we do the same, but instead of the mother  $p_t$  we look at the  $p_t$  fraction of the daughters. The latter is calculated as in the splitting functions, however now we use the minimum  $p_t$  fraction in a split. For this measurement we also use  $\hat{p}_t$  of 300 GeV and a  $\hat{p}_t$  of 500 GeV. This gives one value per split (just like the angle at parton level) between 0 and 0.5. The results are given in Fig. 15. In both generators we see a drop for small  $z$  in the order of  $1/z$  which is comparable with QCD theory. In Pythia however this drop steadily goes on, whereas for Vincia we see again a drop for  $z \rightarrow 0.5$ . Physically this means that both daughters have approximately the same  $p_t$  which thus results in a greater angle between the daughters. From this we can thus deduce that for a more evenly distributed  $p_t$  in a split the angle between the daughters is smaller. Furthermore the angle between the daughters drops  $1/z$  in both generators for small  $z$  and for the whole  $z$ -spectrum in Pythia.

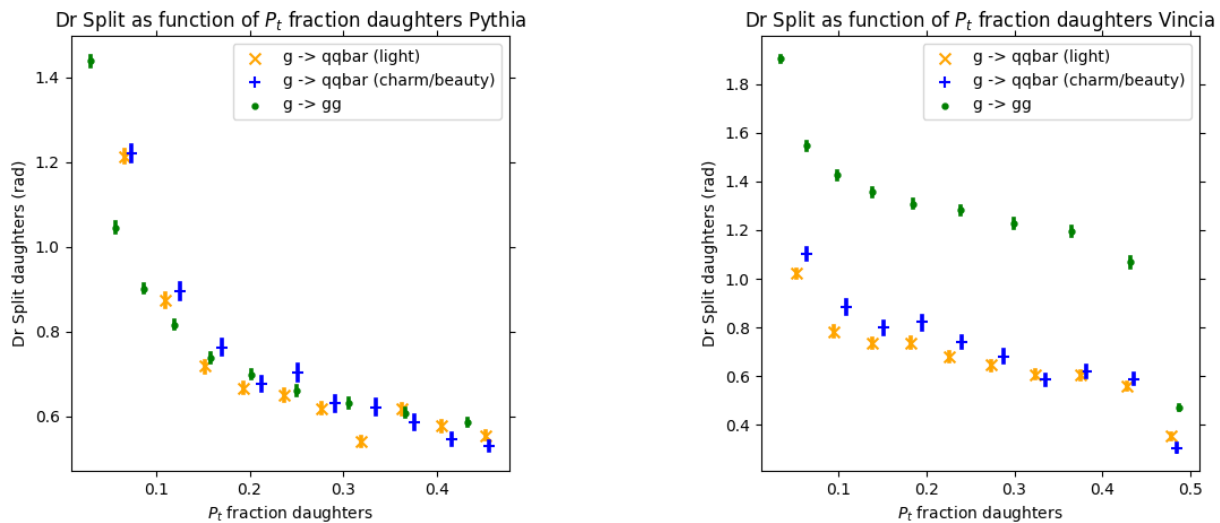


Figure 15: Minimum  $p_t$  fraction ( $z$ ) in a split in a profile plot against the angle at parton level between the daughter particles in Pythia (left) and Vincia (right) for filtered splits. For this we don't fit for clarity reasons. The error bars are standard statistical errors.

## 4.2 Jet level results

Now we will focus our attention on jets. In Sec. 3.2 we described how we match jets to the corresponding daughters. This means that per split we have two matched jets (one to each daughter) if the splitting angle at parton level is greater than  $0.4 = R_{jet}$  (jet radius). Otherwise the daughters are in the same jet and we have one matched jet. Furthermore the determination of the non matched jets are also described in Sec. 3.2. To see if the nonmatched jets are nothing but background radiation we check the  $p_t$  distribution of the nonmatched jets per filtered split. The results are found in Fig. 16.

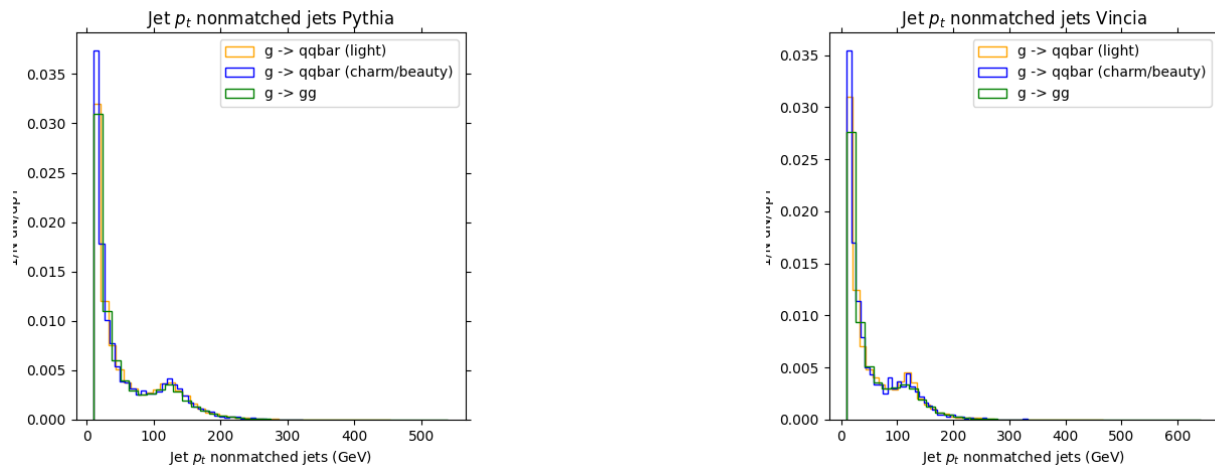


Figure 16: 1D distributions of the  $p_t$  (GeV) of the non matched jets in Pythia (left) and Vincia (right). The two figures show the results for all filtered samples. All histograms are self-normalized and normalized by the bin width.

Once we check the inclusive sample in ROOT, we can see that the distribution for the non-matched jets is similar to the inclusive sample. This means that we cannot simply say that the nonmatched jets are background. If the matched jets have the same  $p_t$  we will save them in a separate file, since we want only matched jets that have different  $p_t$ , i.e. different matched daughters. In this section we focus our attention on 1D histograms. We have results for the jet quantities  $pTD$  jet, jet mass  $M$ , jet width and jet  $p_t$ . The first three observables are explained in Sec. 2.2.2. Since only jet Mass  $M$  and jet width show interesting results we showed the histograms for matched/unmatched jets for  $pTD$  jet in appendix A. Furthermore we will correlate the jet mass, jet width, jet  $pTD$  and jet  $p_t$  to parton quantities in the next section.

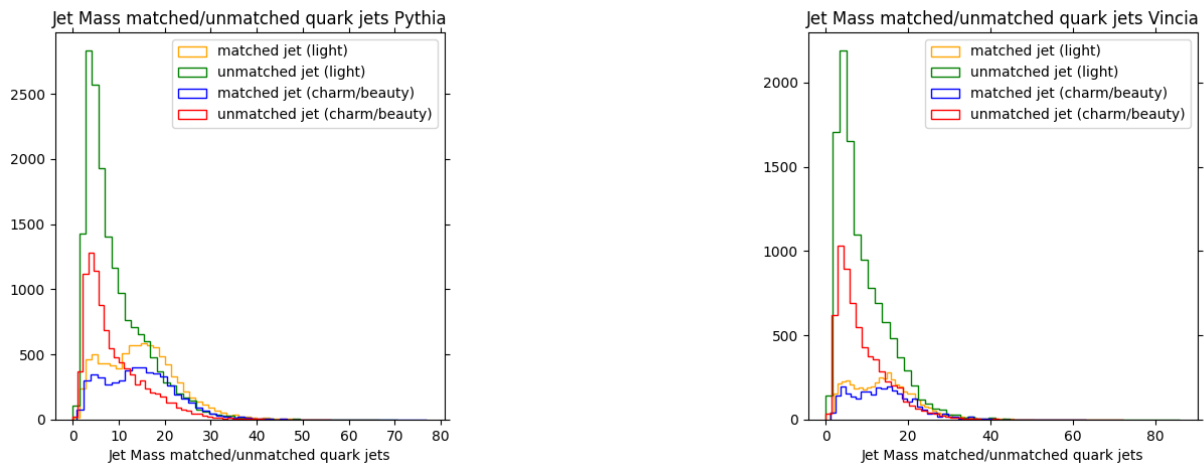


Figure 17: 1D distributions of jet mass in Pythia (left) and Vincia (right). The two figures show the results for quark only splits  $g \rightarrow q\bar{q}$ , where we filter light and heavy quarks separately.

The results of the 1D histograms of the jet mass are found in Fig. 18 and Fig. 17. What we can see in Fig. 17 is that the jet mass for matched jets is a lot more evenly distributed than for unmatched jets. Also we can see that for the unmatched jets on average the jet mass is less than for the matched jets. This means that most of the mass from the daughter stays in the matched jet whereas in the unmatched jet are more lighter particles. This is seen in both Vincia and Pythia.

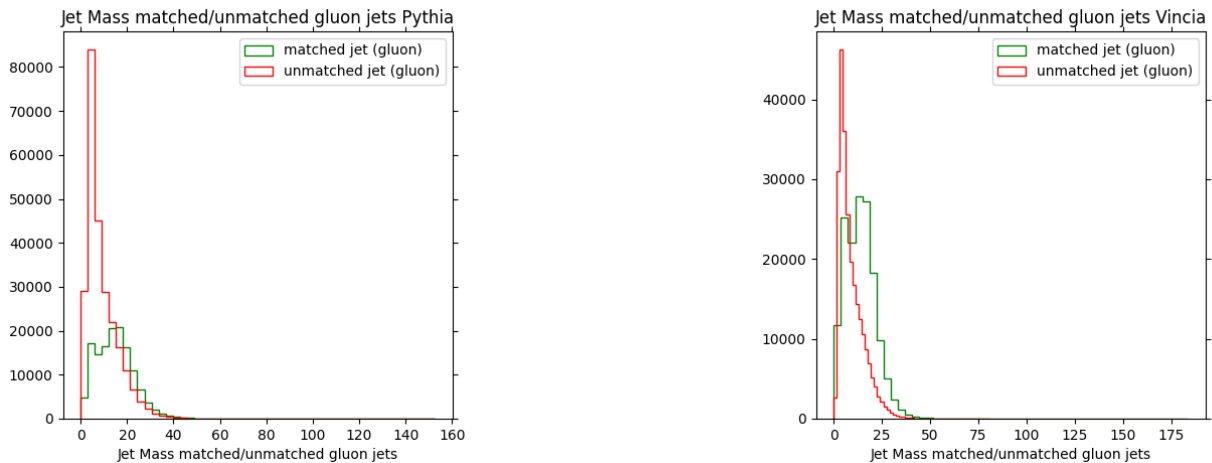


Figure 18: 1D distributions of jet mass in Pythia (left) and Vincia (right). The two figures show the matched/unmatched jet masses for all for  $g \rightarrow gg$  splits.

Furthermore in Fig. 18 we can see the same happening for gluon jets. This means that on average unmatched jets have less mass than matched gluon jets. In Vincia this is a little less clear, but one can see that the peak is shifted a little to the right.



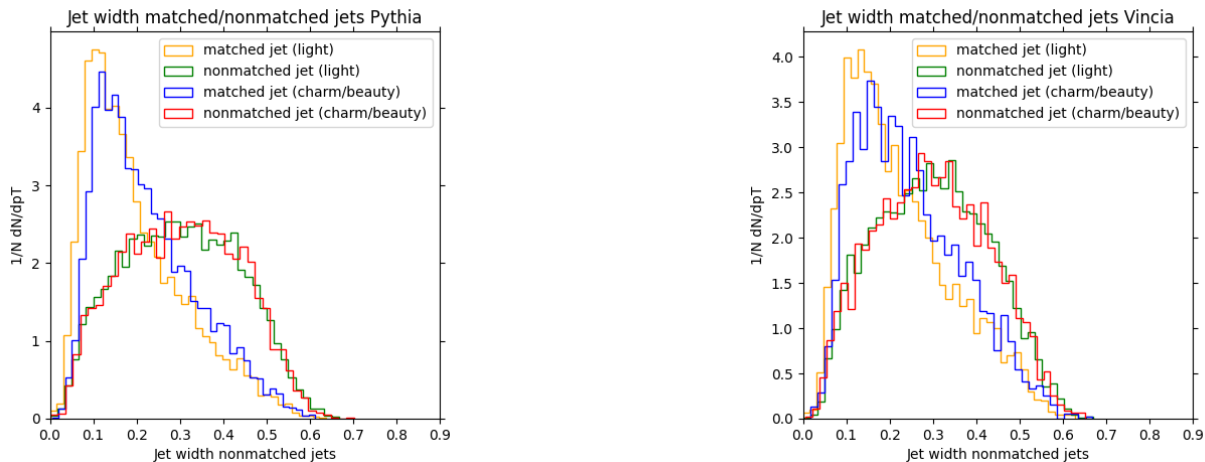


Figure 19: 1D distributions of jet width in Pythia (left) and Vincia (right). The two figures show the results for quark only splits  $g \rightarrow q\bar{q}$ , where we filter light and heavy quarks separately. All histograms are self-normalized and normalized by the bin width.

Next we study the jet width of matched/unmatched jets. The results of the 1D histograms of the jet width are found in Fig. 19 and Fig. 20. What we can see in Fig. 19 is that the jet width for matched jets drops earlier than for unmached jets. If we plot average lines (not done here for clarity reasons) we can see that the average jet width for unmatched jets is somewhat bigger than for matched jets. This means that since daughters carry a lot of momentum to its matched jet, it is perhaps the case that the jet width gets smaller for larger momentum of the matched daughter. We see this happening for both Vincia and Pythia.

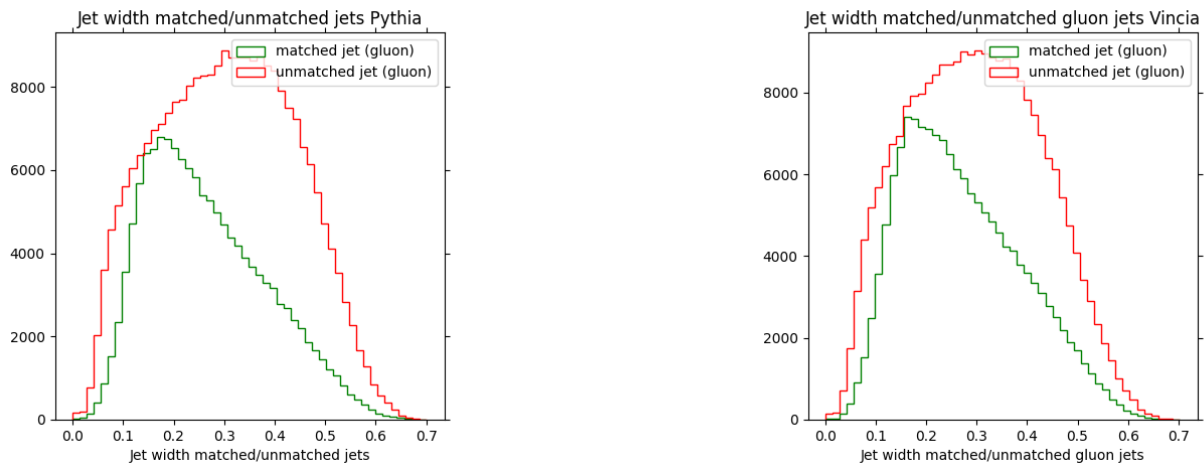


Figure 20: 1D distributions of jet width in Pythia (left) and Vincia (right). The two figures show the matched/unmatched jet width for all for  $g \rightarrow gg$  splits.

Furthermore in Fig. 20 we can see the same happening for gluon jets. This means that on average unmatched jets have a greater jet width than matched gluon jets. In the next section we will check if it is the case that the jet width gets smaller for larger momentum of the matched daughter. We see this happening for both Vincia and Pythia.

In figures 21, 22 are the general results of the matched jets observables width and mass respectively for the different splits. The result for the jet pTD is found in Appendix A in Fig. 29. Looking at both results, we can see that the distribution of  $g \rightarrow gg$  splits is different from  $g \rightarrow q\bar{q}$  splits. On average we see (when drawing an line indicating the average) that the jet width and the jet mass of  $g \rightarrow gg$  is greater than for gluon to quark splits. This means that we can differentiate the two samples from each other by looking at those observables. We did not draw the average line for clarity reasons. Doing the same for the jet pTD gives not the same result, since the distributions are similar and averages overlap.

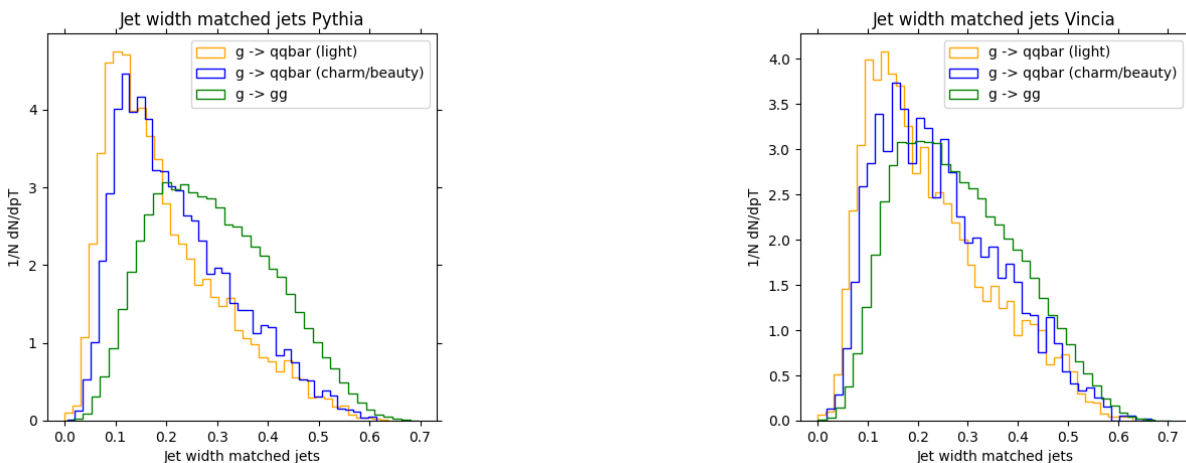


Figure 21: 1D distributions of jet width for matched jets in Pythia (left) and Vincia (right) for all filtered splits. All histograms are self-normalized and normalized by the bin width.

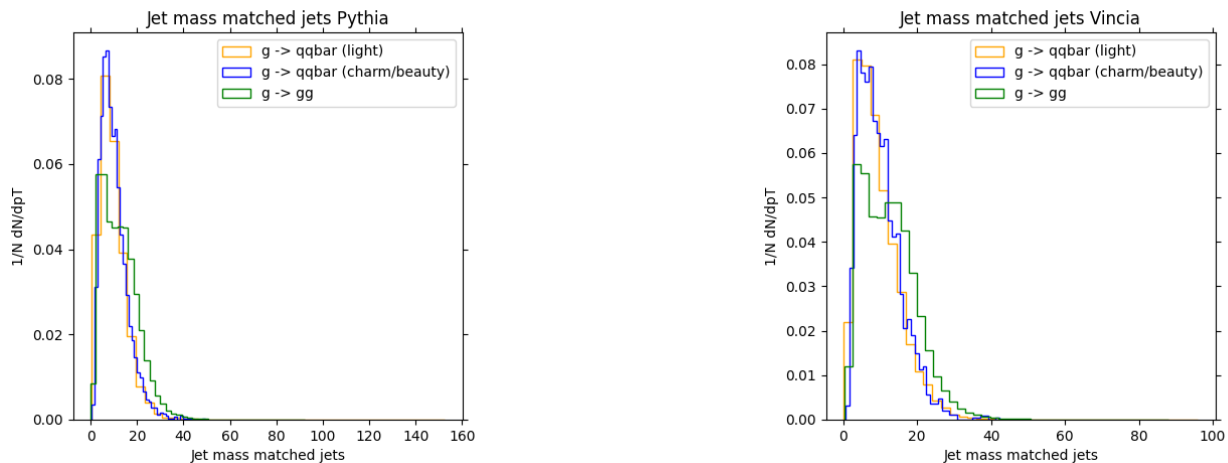


Figure 22: 1D distributions of jet mass for matched jets in Pythia (left) and Vincia (right) for all filtered splits. All histograms are self-normalized and normalized by the bin width.

### 4.3 Parton-Jet correlation results

In this section we correlate different Jet quantities with parton quantities to see if with jet measurements we can say something about what happens on parton level. A lot of quantities were checked but the following were the most interesting. We will consider correlating the angle between the daughters and the angle between the matched jets, the  $p_t$  of the daughters and the jet width of the corresponding matched jets, the  $p_t$  of the daughters and the  $p_t$  of the matched jets and lastly the  $p_t$  of the daughters and the jet mass of the matched jets. The correlation between the matched jet pTD and the  $p_t$  of the corresponding daughter is found in the appendix.

First we check if the angle between the daughters and the angle between its matched jets are correlated. One can think that this is only logical, however a lot can happen in between jets (i.e. momentum loss to other jets).

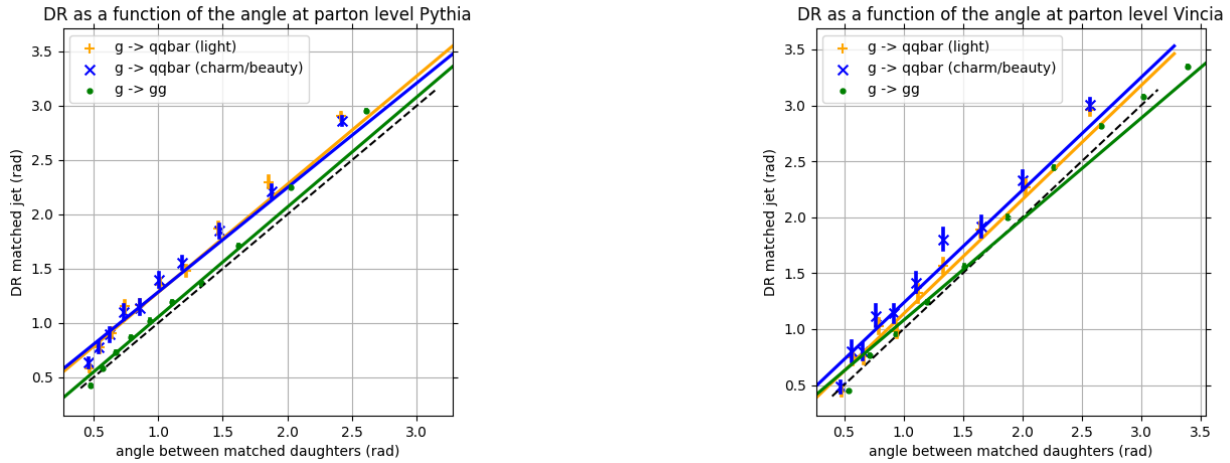


Figure 23: Correlation between the angle between the daughters (rad) and the angle between the corresponding matched jets in Pythia (left) and Vincia (right) for all filtered splits. The error bars are statistical errors. The black dashed lines indicate the diagonal.

The results are shown in Fig. 23. As we can see for both Vincia and Pythia are both positively correlated. This means that for a greater angle between the daughter, is a greater  $\Delta R$  between the matched jets in a split. Thus with jet measurements we can say something about the angle between the two daughter particles. There is not so much error in these measurements since we used all three  $\hat{p}_t$  samples.

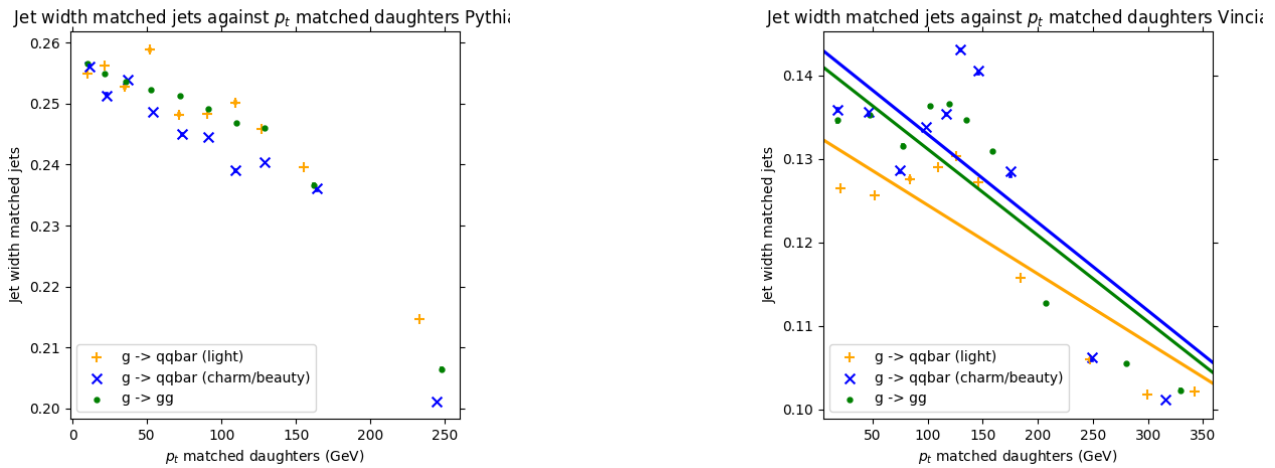


Figure 24: Correlation between the daughter  $p_t$  and the jet width of its corresponding matched jet in Pythia (left) and Vincia (right) for all filtered splits. The error bars are standard statistical errors. There is not so much error in these measurements since we used all three  $\hat{p}_t$  samples. For clarity reasons we did not fit Pythia's measurements.

Next up we correlated the  $p_t$  of the daughters and the jet width of the corresponding matched

jets. The results are shown in Fig. 24. As we can see for both Vincia and Pythia are both negatively correlated. In Pythia it is more clear that from a certain  $p_t$  around 150 GeV we can see that the jet width drops significantly. We also see a decline in Vincia. This means that for a greater daughter  $p_t$ , on average the jet width of its corresponding daughter will be smaller. Thus with jet width measurements we can say something about the  $p_t$  of the daughter particle that is matched to this jet.

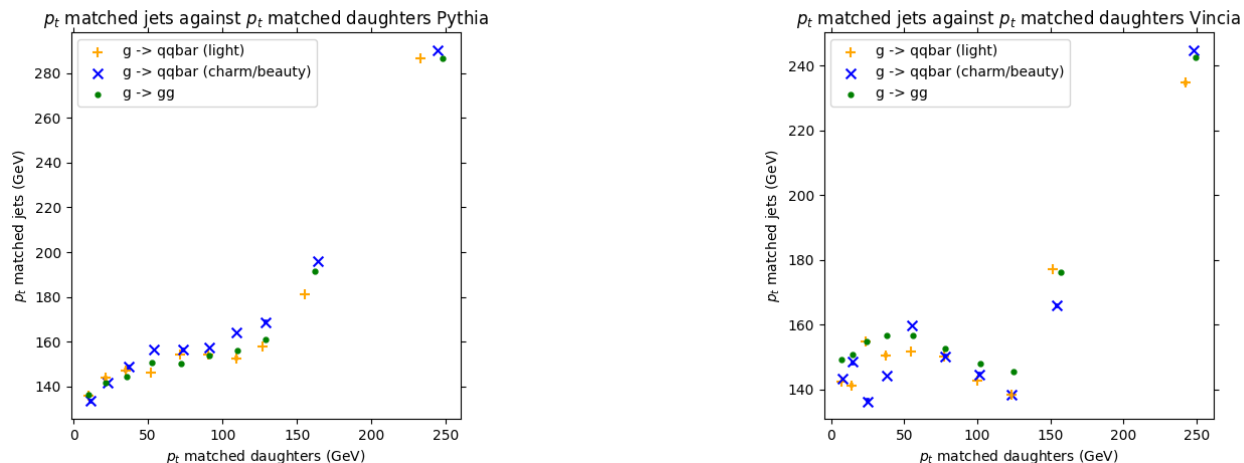


Figure 25: Correlation between the daughter  $p_t$  and the jet  $p_t$  of its corresponding matched jet in Pythia (left) and Vincia (right) for all filtered splits. The error bars are standard statistical errors. There is not so much error in these measurements since we used all three  $\hat{p}_t$  samples. For clarity reasons we did not fit both measurements. The positive correlation is apparent.

Thirdly we correlated the  $p_t$  of the daughters and the jet  $p_t$  of the corresponding matched jets. The results are shown in Fig. 25. As we can see for both Vincia and Pythia are both positively correlated. We can see in Vincia that for the daughter  $p_t$  around 75 GeV the average jet  $p_t$  is twice the momentum. In both generators we can see an interesting polynomial figure appear. At first glance this is not easy to explain. It is therefore interesting to further research this and find theoretical foundation for the shape of this figure.

We also correlated the daughter  $p_t$  to the jet mass of its matched jet. The results are found in 26.

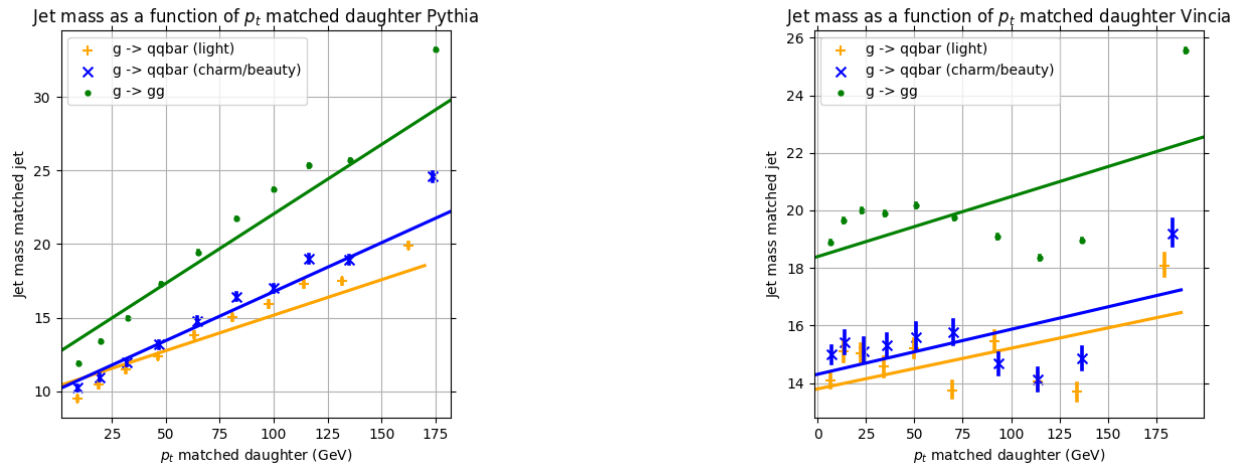


Figure 26: Correlation between the daughter  $p_t$  and the jet mass of its corresponding matched jet in Pythia (left) and Vincia (right) for all filtered splits. The error bars are standard statistical errors. There is not so much error in these measurements since we used all three  $\hat{p}_t$  samples. The positive correlation is apparent for higher  $p_t$ .

We can see from 26 both Pythia and Vincia that those quantities are positively correlated, meaning that for a greater daughter transverse momentum the matched jet had more mass. Also for higher  $p_t$  values for the daughters we saw a great increase in jet mass. This is interesting since the jet width became smaller for higher daughter  $p_t$ . One can conclude from this that for daughters with high  $p_t$  more particles radiate in a smaller cone around it, keeping it in the same jet. This phenomenon is known as jet collimation.

## 5 Conclusion

In this thesis hard scattering events were generated with Pythia8 and Vincia. Different samples with a gluon as the mother particle were compared by filtering light quark splits, charm/beauty quark splits and gluon splits respectively.<sup>2</sup> We distinguish the results in three categories; i.e. parton level, jet level and parton-jet correlation.

First we observed that Vincia can exhibit splits where both daughters have the same PDG whereas Pythia's events are what we expect, namely two daughters with quark flavor but opposite charge. We hypothesized that this has something to do with the NLO calculations made by Vincia. However it also may be a flaw in the way the generator saves different particles.

Next we looked at splitting functions. From Fig. 11 we can see that the events generated with Vincia do not obey the LO kernel splitting functions for  $z \rightarrow 0.5$ . To check the NLO corrections in Vincia we need to follow the NLO radiations in the generator. We do not do this since we only follow two daughters while NLO will result in three.

Before we looked at correlations we checked with 1D histograms the distribution of the splitting angle at parton level for all the filtered splits. None of the filtered splits exhibited odd behaviour, but the  $g \rightarrow b\bar{b}$  split was more evenly distributed. However there are not enough beauty splits to reach firm conclusions.

In addition, we investigated the correlation between  $z$ , the minimum  $p_t$  fraction of the daughters and the angle between them. We calculated the  $p_t$  fraction with the sum of the daughters  $p_t$  since daughters can pick up some initial state radiation resulting in higher transverse momentum than its corresponding mother. We measured for a more evenly distributed  $p_t$  (higher value of  $z$ ) between daughters in a gluon to quark pair split and gluon to gluon pair split that the angle between the daughters is smaller than for less evenly distributed  $p_t$  (lower value of  $z$ ). Furthermore from Fig. 15 we can see that the angle between the daughters drops  $\sim 1/z$  for small  $z$  in both generators and for the whole  $z$ -spectrum in Pythia8.

Lastly we observe in Fig. 14 that a mother parton with higher  $p_t$  is negatively correlated with the angle between its corresponding daughters. This means that for higher mother  $p_t$  we see that the angle between the daughters becomes smaller. We compared Vincia and Pythia samples and saw that for higher  $\hat{p}_t$  we can distinguish easier  $g \rightarrow q\bar{q}$  from  $g \rightarrow gg$  splits using Vincia.

Now on jet level we wrote a small algorithm explained in Sec. 3.2 to distinguish matched/unmatched jets to correlate these with the corresponding daughters and mothers using profile plots. We plotted the average of a jet observable as a function of the  $p_t$  of the matched daughter.

Looking at the results from Fig. 22 and 21 we can see that the distribution of  $g \rightarrow gg$

---

<sup>2</sup>Splits of the sort  $g \rightarrow q\bar{q}$  where  $q$  is  $u, d, s$ ,  $g \rightarrow q\bar{q}$  where  $q$  is  $c, b$  and  $g \rightarrow gg$  respectively.

splits is different from  $g \rightarrow q\bar{q}$  splits. On average we see (when drawing a line indicating the average) that the matched jet width and the matched jet mass of  $g \rightarrow gg$  splits is greater than for gluon to quark splits. This means that we can differentiate the two samples from each other by looking at those observables. We cannot distinguish the quark samples from the  $g \rightarrow gg$  sample by looking at the jet pTD. Also it is quite difficult to distinguish light quarks from heavy quark splits by these observables since their distributions are similar.

Next we observed that the angle between the matched jets and the angle between the corresponding matched daughters is positively correlated. This is interesting since if we observe the angle between matched jets, we would be able to say something about daughters on parton level. Next we saw that for higher daughter  $p_t$  the corresponding jet mass was also higher. Since the jet width became smaller for a higher daughter  $p_t$  one can conclude that more particles are radiated closely around the daughter than for a daughter with lower  $p_t$ , since for the latter both the jet width and the jet mass are less.

Furthermore in Vincia we observe that for daughters with  $p_t < 75$  GeV are on average more found in jets with twice the momentum than daughters with higher  $p_t$ . Finally the shows that the jet width of matched jets drops significantly for higher  $p_t$  values for the matched daughters for all filtered splits in both Pythia and Vincia.

## 6 Discussion and outlook

The first main question was, can we differentiate light quark splits from beauty/charm splits when comparing to the inclusive sample? As seen in the results we did not take the 'whole' inclusive sample into account. We did not look at  $q \rightarrow ab$  splits, but only at  $g \rightarrow ab$  splits. We did this since most of the splits were  $g \rightarrow gg$  to begin with, plus the whole inclusive was too large and segregated to extract sensible results. Also maybe it is an idea to establish some cuts on the sample in for example pseudo-rapidity and  $p_t$  to filter away background noise.

We learned from all the results that it is quite difficult to differentiate light quark splits and charm/beauty splits from the inclusive, at least looking at jet-parton correlations. So maybe comparing Pythia and Vincia is not the way to go. We can however differentiate the quark from gluon sample looking at the jet mass and jet width observable. It is however even more difficult to distinguish heavy quarks from light quark splits since they behave quite similar. Therefore it is perhaps more interesting to use JEWEL and look at Pb-Pb collisions instead of p-p. With this we can incorporate jet quenching and see the different effects on heavy quarks and light quarks from the QGP.

Also for the correlation plots we looked at averages over the whole sample, and not distributions. However in for example Fig. 15 we ran the analysis for 300000 events (for  $\hat{p}_t = 120, 300, 500$  respectively), which is why the statistical error is small. However in the future it is better to generate more events to make the regression plots more accurate. It is also interesting to look at different distributions at fixed values and not just at the regression.



The next main objective of this thesis was to study the differences between Vincia and Pythia. This study had a bit better results. We saw differences looking at the PDG 2D histogram, splitting functions, correlation plots and jet-parton correlation plots. In the right figure in Fig. 8 it is not clear if the 'weird' splits come from fundamental QCD or if Vincia does not correctly save the PDG of the particles. Now looking at the splitting functions we see that Pythia obeys it quite well. The splitting functions were normalized however and translated such that we could only study the shape. As already mentioned it may be also interesting to look at different distributions at fixed values and not just at the regression. In some cases the regression plot showed interesting results, sort of a polynomial dependence. In future research it is interesting to combine theory and these results.

In future research it is interesting to also incorporate  $q \rightarrow ab$  splits and not just gluon splits. One can divide the inclusive sample in all possible quark and gluon splits and compare these two. In addition to this it is interesting to also look at NLO kernel splitting functions for Vincia. Since Vincia has NLO matrix elements it is only logical that these obey the NLO kernel splitting functions. In future research one can repeat this research with JEWEL to incorporate jet quenching to see the effect of the QGP on the initial partons and outgoing jets. With JEWEL we can extend research to heavy ion collisions and not just proton-proton collisions.

## References

- [1] Y.P.Viyogi: *Experimental attempts to detect QGP*  
<https://inis.iaea.org/collection/NCLCollectionStore/Public/24/055/24055298.pdf>
- [2] *Lund string model*  
<https://particle.wiki/wiki/Lundstringmodel>
- [3] *Asymptotic freedom*  
<https://en.wikipedia.org/wiki/Asymptoticfreedom>
- [4] *PYTHIA8*  
<http://home.thep.lu.se/~torbjorn/pythia81html/Welcome.html>
- [5] CERN: *The Standard Model*  
<https://home.cern/science/physics/standard-model>
- [6] Chapter 2 Quark-Gluon Plasma and the Early Universe  
<https://www.physics.umd.edu/courses/Phys741/xji/chapter2.pdf>
- [7] Shanshan Cao, Xin-Nian Wang: *Jet quenching and medium response in high-energy heavy-ion collisions: a review*  
<https://arxiv.org/pdf/2002.04028.pdf>
- [8] CERN: *The Large Hadron Collider*  
<https://home.cern/science/accelerators/large-hadron-collider>
- [9] J. Schukraft: *Heavy-ion physics with the ALICE experiment at the CERN Large Hadron Collider*  
<https://doi.org/10.1098/rsta.2011.0469>
- [10] A. Pich: *Quantum Chromodynamics*  
<https://cds.cern.ch/record/281332/files/9505231.pdf>
- [11] F. Herrmann: *Evolution of Parton Distribution Functions*  
<https://www.uni-muenster.de/imperia/md/content/physiktp/theses/klasen/fherrmannmsc.p>
- [12] Curci, G., W. Furmanski and R. Petronzio: *Evolution of Parton Densities Beyond Leading Order: The Nonsinglet Case* Nucl. Phys., B175:27, 1980.
- [13] Furmanski, W. and R. Petronzio: *Singlet Parton Densities Beyond Leading Order* Phys. Lett., B97:437, 1980.
- [14] T. Renk: *Jet quenching and heavy quarks*  
<https://arxiv.org/abs/1309.3059>
- [15] A. J. Larkoski, J. Thaler and W. J. Waalewijn *Gaining (mutual) information about quark/gluon discrimination*  
[https://doi.org/10.1007/JHEP11\(2014\)129](https://doi.org/10.1007/JHEP11(2014)129)

- [16] The CMS Collaboration *Jet algorithms performance in 13 TeV data*  
<https://cds.cern.ch/record/2256875/files/JME-16-003-pas.pdf>
- [17] S. Marzani, G. Soyez, and M. Spannowsky: *Lecture Notes in Physics (2019)* ISSN 1616-6361  
<http://dx.doi.org/10.1007/978-3-030-15709-8>
- [18] CERN: ROOT  
<https://root.cern>
- [19] The Antenna Shower Model (VINCIA)  
<http://home.thep.lu.se/~torbjorn/pythia83html/Vincia.html>
- [20] *FastJet user manual*  
<http://dx.doi.org/10.1140/epjc/s10052-012-1896-2>
- [21] *FastJet*  
<http://fastjet.fr/>.
- [22] Caron,J.L.(1998): *Overall view of LHC experiments*  
Retrievedfrom<https://cds.cern.ch/record/841555>
- [23] Casalderrey-Solana, J. Can Gulhan, D. Guilherme Milhano, J. Pablos, D. Rajagopal: *A Hybrid Strong/Weak Coupling Approach to Jet Quenching. Journal of HighEnergy Physics* , 19.4-13. DOI:  
[https://doi.org/10.1007/JHEP10\(2014\)019](https://doi.org/10.1007/JHEP10(2014)019)
- [24] M. Schott and M. Dunford: *The European Physical Journal C 74 (2014)*, ISSN 1434-6052  
<http://dx.doi.org/10.1140/epjc/s10052-014-2916-1>
- [25] *Vincia*  
<https://indico.cern.ch/event/432527/contributions/1071535/attachments/1318948/1980058/16-ichep-skandsBuilds.pdf>
- [26] A. Hinzmann and B. Nachman: *Jet substructure measurements with CMS and ATLAS Slide 27*
- [27] G. Aad, B. Abbott, J. Abdallah, S. Abdel Khalek, A. A. Abdelalim, O. Abdinov, B. Abi, M. Abolins, O. S. AbouZeid, H. Abramowicz, et al. , *Physical Review D 86 (2012)*, ISSN 1550-2368  
<http://dx.doi.org/10.1103/PhysRevD.86.072006>
- [28] G. Sborlini, G. Rodrigo, D. Florian *Double collinear splitting amplitudes at next-to-leading order*  
DOI:10.1007/JHEP01(2014)018

## A Appendix A

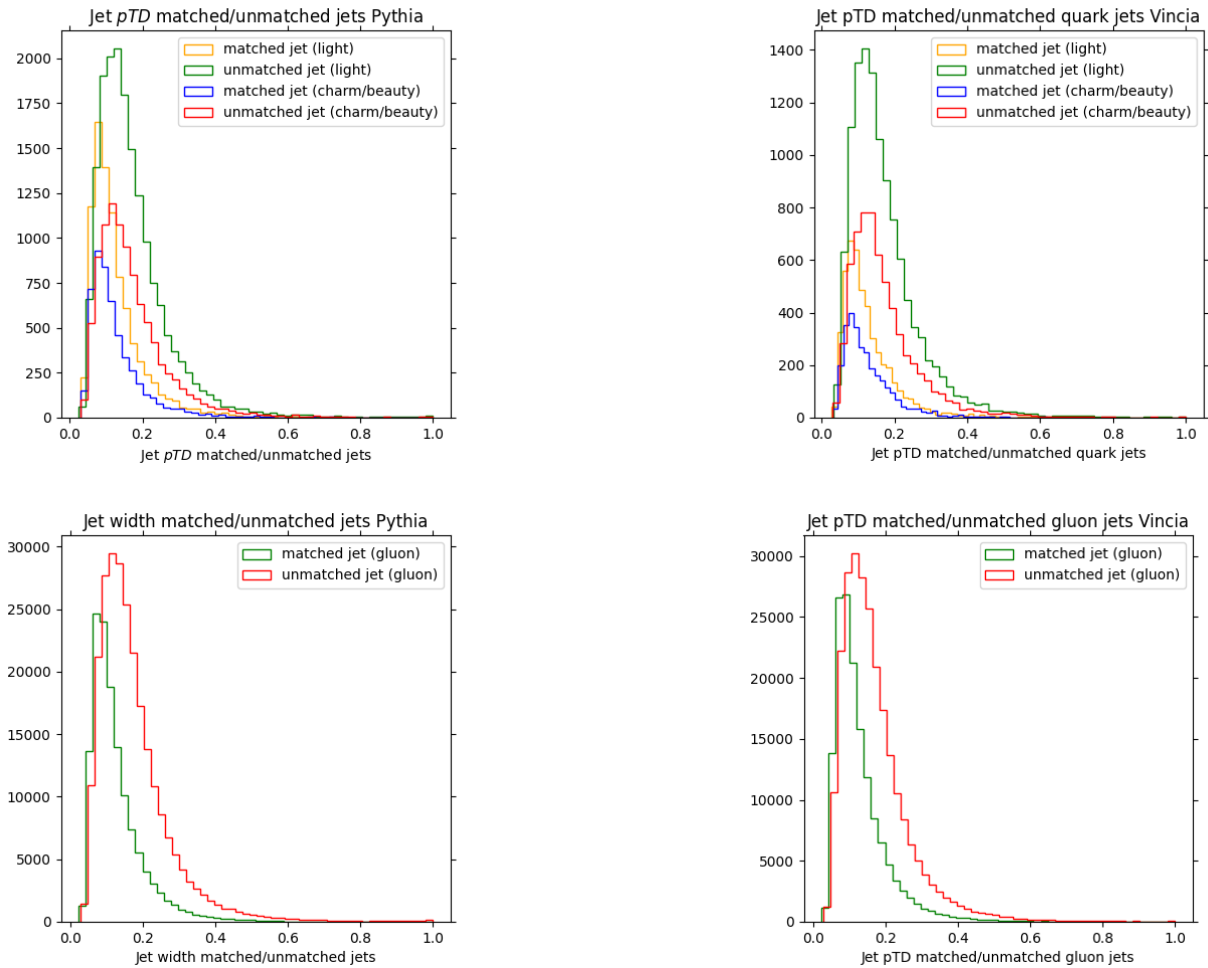


Figure 27: 1D distributions of jet pTD for matched/unmatched jets in Pythia (left two figures) and Vincia (right two figures). The top two figures show the results for quark only splits  $g \rightarrow q\bar{q}$ . The bottom two show the results for all for  $g \rightarrow gg$  only.

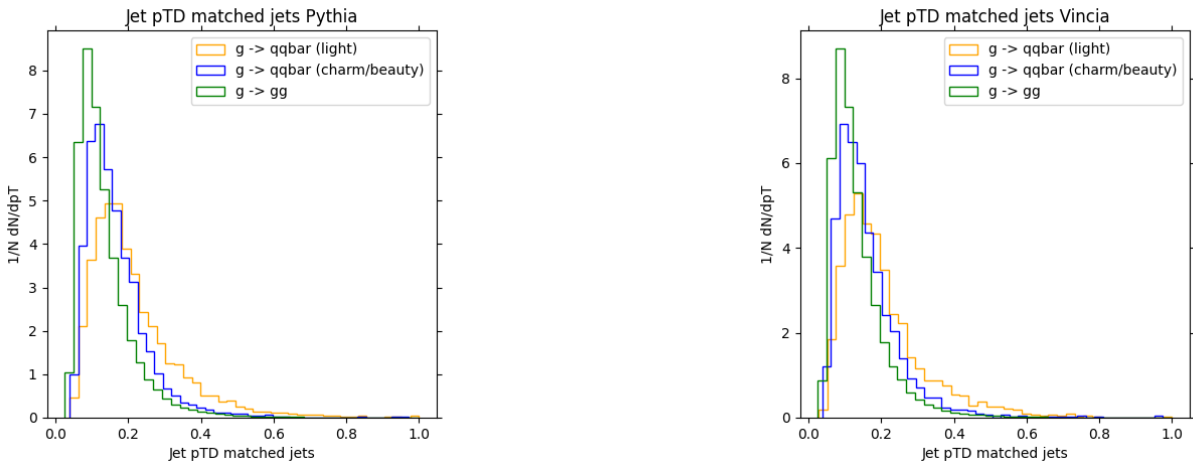


Figure 28: 1D distributions of jet pTD for matched jets in Pythia (left) and Vincia (right) for all filtered splits. All histograms are self-normalized and normalized by the bin width.

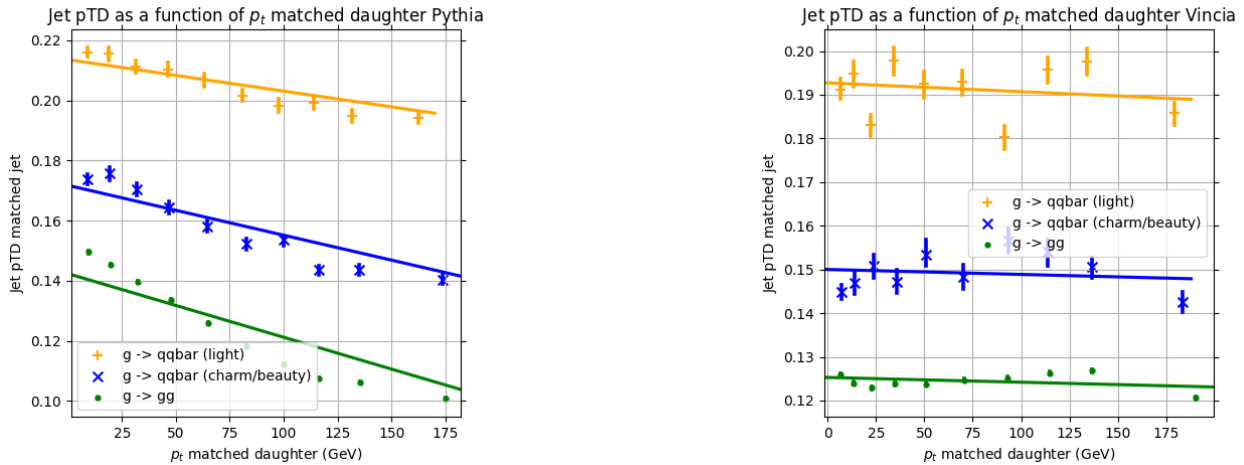


Figure 29: Correlation between the daughter  $p_t$  and the jet pTD of its corresponding matched jet in Pythia (left) and Vincia (right) for all filtered splits. The error bars are standard statistical errors. There is not so much error in these measurements since we used all three  $\hat{p}_t$  samples. We can observe that there is a small negative correlation, however not significant to discuss.